AD_____

Award Number: DAMD17-98-1-8594

TITLE: Targeted Radioimmunotherapy of Prostate Cancer Using Monoclonal Antibodies to the Extracellular Domain of Prostate-Specific Membrane Antigen

PRINCIPAL INVESTIGATOR: Shankar Vallabhajosula, Ph.D.

CONTRACTING ORGANIZATION: Cornell University Medical College
New York, New York 10021

REPORT DATE: November 2000

TYPE OF REPORT: Final, Phase I

PREPARED FOR: U.S. Army Medical Research and Materiel Command
Fort Detrick, Maryland 21702-5012

REPORT DOCUMENTATION PAGE

Form Approved
OMB No. 074-0188

1. AGENCY USE ONLY (Leave blank)	2. REPORT DATE	3. REPORT TYPE AND DATES COVERED
	November 2000	Final, Phase I (1 Jun 98 - 30 Nov 00)

4. TITLE AND SUBTITLE
Targeted Radioimmunotherapy of Prostate Cancer Using Monoclonal Antibodies to the Extracellular Domain of Prostate-Specific Membrane Antigen

5. FUNDING NUMBERS
DAMD17-98-1-8594

6. AUTHOR(S)
Shankar Vallabhajosula, Ph.D.

7. PERFORMING ORGANIZATION NAME(S) AND ADDRESS(ES)
Cornell University Medical College
New York, New York 10021

E-MAIL:
svallabh@med.cornell.edu

8. PERFORMING ORGANIZATION REPORT NUMBER

9. SPONSORING / MONITORING AGENCY NAME(S) AND ADDRESS(ES)
U.S. Army Medical Research and Materiel Command
Fort Detrick, Maryland 21702-5012

10. SPONSORING / MONITORING AGENCY REPORT NUMBER

11. SUPPLEMENTARY NOTES
This report contains colored photos

12a. DISTRIBUTION / AVAILABILITY STATEMENT
Approved for public release; distribution unlimited

12b. DISTRIBUTION CODE

13. ABSTRACT *(Maximum 200 Words)*

The purpose of this research proposal was to evaluate the potential diagnostic and therapeutic value of radiolabeled monoclonal antibodies (J591, J533, J415) specific to the extracellular domain of PSMA ($PSMA_{ext}$). We previously reported all the in vitro studies and some preliminary biodistribution and radioimmunotherapy studies in nude mice. This final report describes all the in vivo studies including biodistribution and radioimmunotherapy evaluations. The pharmacokinetics, biodistribution, and tumor uptake of ^{131}I and ^{111}In-labeled MAbs were performed in nude mice bearing LNCaP tumors. There were significant differences in the absolute tumor uptake (%ID/g) among the ^{131}I MAbs. By contrast, the tumor uptake of ^{111}In and ^{177}Lu labeled MAbs was similar. However, the T/B and tumor/muscle (T/M) ratios were significantly higher with ^{111}In and ^{177}Lu compared to ^{131}I-MAbs. In addition, the ratios were significantly higher with J591 and J415 compared to that of 7E11 (antibody specific to intracellular domain of PSMA). Radioimmunotherapy studies with ^{131}I-J591, ^{90}Y-DOTA-J591, and ^{177}Lu-DOTA-J591 produced an unambiguous dose-response resulting in tumor shrinkage or slowing the growth over a period of 4-6 weeks. The most important finding is that this therapeutic response was specific since ^{90}Y-non-specific MAb had no response. These results clearly demonstrate that radiolabeled MAbs specific $PSMA_{ext}$ are useful for RID and RIT of prostate cancer.

14. SUBJECT TERMS	15. NUMBER OF PAGES
Prostate Cancer, Radiolabeled antibodies, Radioimunotherapy	45
	16. PRICE CODE

17. SECURITY CLASSIFICATION OF REPORT	18. SECURITY CLASSIFICATION OF THIS PAGE	19. SECURITY CLASSIFICATION OF ABSTRACT	20. LIMITATION OF ABSTRACT
Unclassified	Unclassified	Unclassified	Unlimited

Table of Contents

INTRODUCTION

The prostate specific membrane antigen (**PSMA**), is a well characterized integral membrane glycoprotein, expressed in a highly restricted manner by prostate epithelial cells. PSMA is expressed by a very high proportion of PC and this expression is augmented in higher grade cancers, in metastatic disease, and in hormone-refractory PC. Therefore, we hypothesized that a radiolabeled MAb specific to the extracellular domain of PSMA ($PSMA_{ext}$) on viable PC cells, is ideal for in vivo prostate specific targeting strategies and would provide benefits, including improved localization and greater potential for radioimmunodiagnosis (RID) and radioimmunotherapy (RIT). In 1997, Bander and his colleagues in our institution reported the development of four IgG MAbs (J591, J533, J415, E99) to the $PSMA_{ext}$. Immunohistochemical studies showed excellent reactivity with PC cells. The pilot studies with ^{131}I- and ^{111}In-labeled MAbs and competitive binding assays (CBA) with LNCaP cells demonstrated that J591 has higher reactivity to PSMA than CYT-356 (ProstaScint, imaging agent), which binds to cytoplasmic domain of PSMA.

The purpose of Phase I research proposal was to evaluate the potential diagnostic and therapeutic value of PSMA-specific MAbs and their fragments radiolabeled with γ- (In-111), β^- (I-131, Y-90) and α emitting radionuclides (Bi-212 or Bi-213). The specific objectives were:

- To optimize radioiodination techniques of MAb and fragments with I-131 and to optimize radiolabeling of MAb and their fragments with In-111, Y-90, Bi-212 using bifunctional chelating agents such as DOTA.
- To evaluate the relationship between specific activity and immunoreactivity of radiolabeled preparations using competitive binding assays and autoradiography.
- To study the biodistribution and tumor uptake of several radiolabeled MAb preparations and to identify the most suitable preparation(s) for diagnostic and therapeutic studies.
- To evaluate and compare the therapeutic response of several radiolabeled MAb preparations in nude mice bearing PSMA positive LNCaP tumors.
- To identify the most appropriate MAb radiolabeled with a β^- emitting radionuclide for subsequent clinical trials in patients with prostate cancer (phase 2 research proposal).

The Statement of Work (SOW) in the original research proposal consisted of six different phases. We previously reported (**The First Annual Report** and **18-Month Competitive Progress Report**) all the in vitro studies and some preliminary biodistribution and radioimmunotherapy studies in nude mice. This final report describes a summary of all the research effort for the entire funding period of the Phase I research proposal.

BODY

The Statement of Work (SOW) in the original research proposal consisted of six different phases. Based on experimental results, relatively minor changes were made in various tasks as originally planned, but the experimental design as originally planned was implemented. We previously reported (The First Annual Report and 18-Month Competitive Progress Report) all the in vitro studies and some preliminary biodistribution and radioimmunotherapy studies in nude mice. This final report describes a summary of all the research effort for the entire funding period of the Phase I research proposal.

Phase 1: Radiolabeling MAbs and in vitro studies:

The techniques of radiolabeling MAbs (J591, J415, J533) and fragments with different radionuclides (^{131}I, ^{111}In, and ^{90}Y) was optimized to achieve a specific activity of 5-10 mCi/mg and yet preserve >70% immunoreactivity. Radiolabeling MAb E99 was not successful and further work with this antibody was discontinued. Compared to DTPA method, DOTA conjugation of MAbs resulted in higher stability of ^{111}In and ^{90}Y labeled complexes. An average of 5 DOTA molecules could be randomly conjugated to J591 and J415 antibodies with little apparent loss of immunoreactivity. Both these antibodies could be efficiently labeled with ^{111}In or ^{90}Y (5-10 mCi/mg). Immunoreactivity of radiolabeled antibody preparations (determined using Lindmo method) was >75%. A direct comparison of the chelate stability of ^{111}In-DTPA-7E-11 and ^{111}In-DOTA-J591 showed that ^{111}In was lost from DTPA-7E-11 with an apparent half-life of 11 hours, whereas the DOTA chelate had an apparent half-life exceeding 1000 hours (**Appendix-A; Figure-3**).

In vitro characterization of radiolabeled J591, J415 and J533 MAbs:
Competitive binding studies with PSMA positive and PSMA negative cell lines (both viable and permeabilized) demonstrated very interesting and **unique** PSMA binding characteristics of radiolabeled MAbs. We have demonstrated clearly that there is no cross-competition between J591, J415, and J533 MAbs specific to $PSMA_{ext}$ and 7E11 MAb that is specific to the internal domain of PSMA. We also demonstrated that J591 and J415 bind to the same epitope of PSMA while the binding site for J333 appears to be a different region (epitope) of PSMA. (**Appendix-A; Figure-4A-C**). ^{131}I-J415 could be displaced from binding to LNCaP cell membranes by both J415, J591 and not J533 (Figure 4A). ^{131}I-J591 binding could be displaced by J591 and J533, but not J415 (**Figure-4B**). ^{131}I-J591 binding could be displaced by J591, J415 and J533 (**Figure-4C**). Among these three antibodies, The IC_{50}s of J591(3.1±1.5 nM) and J415 (1.3±0.9 nM) were lower compared to that of J533 (7.7±5.5) suggesting that the affinity of J533 to PSMA is less than that of either J591 or J415.

Saturation binding studies of ^{131}I-J591 or ^{131}I-J415 to LNCaP viable intact cells (**Appendix-A; Figure –5**) showed a characteristic high affinity (K_d = 1.8± nM) binding of an antibody to a single class of antigen (600,000 – 800,00 sites/cell). In contrast, J533 had lower affinity (K_d = 18±5 nM). In parallel studies, these three antibodies bound to a similar number of PSMA sites expressed by permeabilized (ruptured) cells. In contrast, ^{131}I-7E-11 specifically bound to only 10-15% of the PSMA sites expressed by intact cells. With ruptured cells, 7E-11 binding, however, was similar to that of J591 (**Appendix-A; Figure-6**). Similarly, autoradiographic

studies performed on LNCaP tumor sections also showed that binding of J591 and J415 is very specific to the external domain of PSMA and there was no cross competition with 7E11 (data reported in the First Annual Report).

Phase II and III: Pharmacokinetics, Biodistribution and Tumor Uptake Studies:

The pharmacokinetics, biodistribution, and tumor uptake of ^{131}I and ^{111}In- labeled MAbs were performed in nude mice bearing LNCaP tumors. As a control, similar studies were performed with a radiolabeled non-specific antibody.

Tumor Model

Prostate carcinoma cell lines LNCaP, DU145 and PC3 (American Type Culture Collection, Rockville, MD) were grown in RPMI 1640, supplemented with 10% fetal calf serum, at a temperature of 37°C in an environment containing 5% CO_2. Prior to use, the cells were trypsinized, counted and suspended in Matrigel (Collaborative Biomedical Products, Bedford, MA). Nu/Nu BalbC mice 8-10 weeks of age were inoculated, in the right and left flanks, with a suspension of 5 x 10^6 LNCaP cells in Matrigel. After a period of 14-18 days, tumors (100-200 mg) had developed. In eight animals, DU145 and PC3 cells were implanted in an identical way.

Biodistribution Studies:

Tumor bearing mice were injected, via the tail vein, with 80KBq of the iodinated MAb (400 MBq/mg) in 200 µL of PBS (pH 7.4, 0.2% BSA). Groups of animals were sacrificed after 2, 4 or 6 days and the major organs and tumors recovered. These samples were weighed and counted, with appropriate standards in an automatic NaI(Tl) counter. These measured relative activity data (cpm) are background corrected and expressed as a percentage of the injected dose per gram (%ID/g). These data were also fitted with a least squares regression analysis (Microcal Origin, Northampton, MA) to determine the biological clearance of the various agents. Based on initial evaluation of organ uptakes, J415, J591 and 7E11 were labeled with ^{111}In (100MBq/mg). 80 KBq of the In-111 version of these MAbs was injected in groups of animals. Subsequent handling was similar for the I-131 MAb injected animals. The derived data was used to determine the residence times for the ^{131}I and ^{111}In labeled antibodies. Using the biodistribution data of ^{111}In as a surrogate for ^{90}Y and ^{177}Lu labeled antibodies the residence times for these radiolabeled MAbs were also determined.

The biodistribution of ^{131}I-J591 and ^{131}I-J415 was compared to that of a non-specific antibody (anti B1 antibody (**Table-1**). At one day post injection, tumor uptake of radiolabeled J591 and J415 is 2-3 times that of non-specific antibody while the blood activity for all the antibody preparations was similar suggesting that tumor uptake of J591 and J415 is specific. By two days post injection (**Table-2**), all the iodinated PSMA-specific MAbs had similar tumor accumulations except for J533. The tumor to blood ratios at day two showed that J533 was significantly lower than J415, J591 or 7E11. Similar results were seen at day 4 (**Table-3**). Compared to radioiodinated antibodies, ^{111}In labeled antibodies show an elevated uptake in liver and spleen. At six days post injection (**Table-4**), the tumor values were similar for ^{111}In labeled J591, J415 and 7E11, but the activities in the other organs, especially the blood, varied considerably. For both ^{111}In and ^{131}I forms of J415 and J591, the blood clearance was significantly faster than 7E11, with the day six values being about 50 % those of 7E11. The

tumor uptakes of the ^{111}In labeled MAbs was remarkably similar at six days post injection. The ^{131}I MAb tumor uptake was systematically lower than the corresponding ^{111}In labeled MAbs and probably reflects the internalization of the MAbs and their cellular metabolism. Consequently, the highest tumor/blood ratios were obtained with the^{111}In labeled J415 and J591 at six days post injection.

There were significant differences in the absolute tumor uptake (%ID/g) among the ^{131}I MAbs. On day 6, J591 (9.6± 2.2%) was significantly less than that of J415 (15.4± 2.4) and 7E11 (14.5± 4.8). By contrast, the tumor uptake of ^{111}In labeled MAbs was similar and was approximately 17% of ID/g. However, the T/B and tumor/muscle (T/M) (**Appendix-B; Figure-1**) ratios were significantly higher with ^{111}In compared to radioiodinated antibodies. In addition, the ratios were significantly higher with J591 and J415 compared to that of 7E-11. For example, on day 6, the T/B with ^{111}In-DOTA-J591 (6.1± 1.8) was 2-3 times compared to that of ^{131}I-J591 (2.3±0.8). In comparison, the T/B and T/B ratios with J533 (data not shown) were much lower. Significant differences in the rate of radioactivity clearance from the blood and other non-target organs was seen with J415>J591>7E11=J533. The tumor uptake of ^{131}I-J591 in mice bearing PSMA-negative PC3 or DU145 tumors was significantly lower ($p<0.01$) than in mice bearing LNCaP tumors. At 4 days post injection, the PC3 tumors (n=10) had an uptake of 0.66 ±0.07 % ID/g and the DU145 tumors (n=6) 0.55 ±0.03 %ID/g compared to 11.4 ±1.49 % ID/g for LNCaP.

Preliminary studies with ^{131}I labeled J591 fragments indicated that the tumor uptake (at 48 hrs) of the labeled fragments was significantly less that that of intact antibody; 4.93±1.25 with $F(ab')_2$ and 1.71±0.53 with Fab' compared to 9.58±2.16 with intact J591. While the T/B and T/M ratios were slightly higher initially compared to intact antibody, the kinetics of washout were not favorable.

Imaging studies:

Animals were injected with 2 MBq ^{111}In-DOTA-J591. At 1, 2, 3, 4 and 6 days post injection, they were sedated with ketamine/xylazine 100 mg/kg/10 mg/kg IP and imaged with a ADAC Transcam gamma camera (ADAC Laboratories, Milpitas, CA) equipped with a pinhole collimator. Data were collected for a gamma energy of 245 keV with a 20 % window for 1000 seconds using a 256 x 256 matrix. Gamma camera images of the same animal, obtained up to 6 days post injection are shown in **Appendix-B; Figure-2.** After one day, the single tumor (250 mg) is easily visualized on the right hind quarter and the blood pool and liver are observed. In the later images, the activity is seen to clear from the blood and the tumor accumulation become more intense. The biodistribution studies based on counting tissue samples at various times post injection provided more quantitative data for comparison of antibodies compared to imaging studies of mice at several times post injection. Therefore, imaging studies were not performed for all the radiolabeled antibody preparations.

^{177}Lu-DOTA-J591:

In this research project, we originally did not plan to evaluate the potential therapeutic value of ^{177}Lu antibodies. However, we wanted to study the relative advantages of this ^{177}Lu labeled

antibodies compared to that of ^{90}Y labeled antibodies. **These studies are absolutely new** and were not included in the original SOW.

For targeted radioimmunotherapy of prostate cancer, huJ591 monoclonal antibody could be labeled efficiently with several radionuclides (^{131}I, ^{90}Y, ^{177}Lu) emitting beta particles. Among the 3 potentially useful radionuclides, I-131 labeled antibody is relatively unstable in vivo due to dehalogenation while Y-90 and Lu-177 labeled antibodies are quite stable in vivo. Y-90 radionuclide has very high energy beta particles with several mm range in tissue and has been investigated in many clinical trials in the last 10 years. While Y-90 nuclide can deliver higher radiation dose to tumor, the main toxicity may be due to bone marrow. As a result, administration of optimal doses of Y-90-HuJ591 may not be possible. The higher beta energy particles may be good for bulky tumors, but it may not be necessary for small tumors. In contrast, Lu-177 has low energy beta particle with only 0.2-0.3 mm range and delivers significantly less radiation dose to marrow compared to Y-90. In addition, due to longer physical half-life, the tumor residence times are higher. As a result, higher activities (more mCi amounts) of ^{177}Lu-J591 can be administered with comparatively less radiation dose to marrow. Lu-177 has been evaluated in several clinical and pre clinical trials as a potential therapeutic agent for radioimmunotherapy of ovarian and bone cancer.

The kinetics of biodistribution and tumor uptake of ^{177}Lu-DOTA-J591 was compared to that of ^{111}In-DOTA-J591 in nude mice bearing LNCaP tumors (**TABLE-5**). At 4 days post injection, the tumor uptake of ^{177}Lu was greater than that with ^{111}In (19.3±4.3 vs. 15.7±1.3). The tumor/blood ratios were slightly better with ^{177}Lu. The kinetics of blood clearance and tumor uptake of ^{177}Lu-DOTA-J591 was compared to both ^{111}In-DOTA-J591 and ^{131}I-J591 (**Appendix-B; Figure-3A and 3B**). While the blood activity of these three tracers was similar, the tumor uptake of ^{177}Lu-DOTA-J591 was significantly greater compared to other two tracers. These results clearly suggest the potential advantages of ^{177}Lu labeled antibodies for RIT studies.

Phase IV: RIT of Prostate Cancer: Studies in tissue culture:

Internalization and cellular processing of radiolabeled antibodies was studied in order to understand the relative advantages of ^{111}In labeled MAbs over ^{131}I labeled MAbs for RIT studies. LNCaP cells in a petri dish were incubated with ^{131}I and ^{111}In labeled J591 and J415 antibody preparations. The cells were incubated for 1 hr with radiolabeled J591or J415. The unbound activity was removed and the labeled cells washed to remove any unbound radioactivity and fresh medium was added. Over the next 2 days, the % of cell bound activity was determined at several time points. The kinetics of wash out and the net cell associated activity was determined. With both antibodies, the net retention of ^{131}I activity was 30% compared to 70-90% retention with ^{111}In (**Appendix-A; Figure-7**). With J415, however, the kinetics of washout of both ^{131}I and ^{111}In activity from the cell was faster compared to radiolabeled J591. These studies suggest that the intracellular metabolism of these two MAbs is different. In addition, MAbs labeled with ^{90}Y would be more effective for radiotherapy, since the net retention of radioactivity is greater with ^{111}In compared to ^{131}I-MAbs.

In a different study, the kinetics of uptake of ^{111}In labeled J591 and J415 was compared to that of 7E-11. LNCaP cells were incubated with ^{111}In labeled antibody preparations and % of added activity associated with cells at various times over the next 2 days was determined. With J591

and J415, the initial cellular uptake rate of ^{111}In activity was 10-20 times faster than that of 7E-11. Over the next 2 days, significantly more ^{111}In activity was associated with cells with J591 compared to J415. In contrast, the no significant uptake of ^{111}In activity was seen with 7E-11 antibody (**Appendix-A; Figure-9**).

Phase V and VI: RIT of Prostate Cancer: Studies in nude mice with LNCaP tumors

Based on in vitro and in vivo characterization of radiolabeled MAbs specific to PSMAext, 4 (four) β- emitting radiolabeled antibody formulations (^{131}I-J591, ^{90}Y-DOTA-J591, ^{90}Y-DOTA-J415, ^{177}Lu-DOTA-J591) have been selected for evaluating the therapeutic efficacy of RIT in nude mice bearing LNCaP tumors.

Method:
Over a period of 18 months, 6 experiments were performed evaluating the efficacy of RIT with Radiolabeled MAbs (**Table-6**). Nude mice bearing LNCaP tumors (50-100 mg or 400-800 mg) were divided into several groups (6-8 mice group). In each experiment, the test groups of mice received different doses of radiolabeled MAb by the tail vein. Some groups of mice received repeat injections of the dose 2-3 times over a period of 2 months. Animals were periodically weighed and tumor dimensions determined over a period of 2-4 months. The response to the treatment was compared to a control group of mice that received no treatment. Mice were sacrificed if the tumor burden exceeded 10% of body mass or if the body mass decreased by 20% compared to baseline value. Typically, the control group of mice experienced uncontrolled tumor growth and a steady decline in body mass. These animals had a median survival time of 6 weeks. The mice that received radiolabeled MAb preparation, showed a delay in tumor growth or a reduction in tumor size.

RIT experiment 1: 4 groups of mice (5 mice/group) with 250-400 mg of tumors were included in this study. (Table-6). The control group received no treatment. The three test groups (2-4) received ^{131}I-J591; 100μCi by the tail vein, 100μCi intraperitoneally and 300μCi by the tail vein. Compared to untreated controls, anti-tumor effect of ^{131}I-J591 was dependent on the dose. At 100μCi dose, there was some delay and reduction in tumor size. But at 300μCi dose, all the mice had a significant reduction (>30%) in tumor size. 2/5 mice in the control group died in 4 weeks while the remaining survived more than 6 weeks. With I-131 there was no improvement in % survival rate. However, mice that received 100μCi dose intraperitoneally survived more than 6 weeks (**Appendix-B; Figure-4**).

RIT experiment 2: 4 groups of mice (5 mice/group) with 250-400 mg of tumors were included in this study. (Table-6). The control group received no treatment. Group-2 received ^{131}I-J591 (300μCi); groups-3 received a single 30μCi dose of ^{90}Y-DOTA-J591 while group-4 received 2 doses (day 0 and day 21). Compared to the control group both ^{131}I-J591 and ^{90}Y-DOTA-J591 showed a 20-30% reduction in tumor size (**Appendix-B; Figure-5A**). In the control group, there was a gradual reduction (20% within 6-8 weeks) in the total body mass associated with the uncontrolled tumor growth. Similar reduction in body mass was seen with a single 30μCi dose of ^{90}Y-DOTA-J591. However, mice that received a second injection of the treatment dose showed a gradual increase in body mass. With ^{131}I-J591, there was some recovery of body mass, but the mice died within 8-10 weeks (**Figure-5B**).

RIT experiment 3: 5 groups of mice (5-7 mice/group) with 250-400 mg of tumors were included in this study. (**Table-6**). The control group received no treatment. A second control group received a 30μCi dose of ^{90}Y-DOTA-F23 (a non-specific antibody). Three other groups of mice received 3 different doses of ^{90}Y-DOTA-J591 (30, 60, and 90μCi). The mice in these three groups received repeat injections at the same dose level 3 times (day 0, 28, and 56). The mice in the second control group that received a non-specific antibody also had an uncontrolled tumor growth similar to the mice that received no treatment. The anti-tumor effect (decrease in tumor size) of ^{90}Y-DOTA-J591 was dose dependent; 30% at 30μCi , 50-70% at 60μCi , and >70% reduction at 90μCi dose level (**Appendix-B; Figures-6A and 6B**). Mice that received 30 and 60μCi doses showed a significant prolongation of survival compared to control groups. 90μCi dose has a shorter survival and appears to be more toxic than 30-60μCi dose levels. In the control group, there was a gradual reduction (20% within 6-8 weeks) in the total body mass associated with the uncontrolled tumor growth. Mice that received repeated treatment doses of 30-60μCi of ^{90}Y-DOTA-J591 showed a gradual increase in total body mass (**Figure-6C**).

RIT experiment 4: 3 groups of mice with LNCaP tumors (400-800 mg) were injected with 3 different doses (150, 200, 300μCi) of ^{90}Y-DOTA-J591. All the mice received only a single treatment dose. There was a significant reduction in tumor size at all 3 dose levels. However, at 150μCi dose level, tumors started growing again after 5 weeks. In contrast, most of the mice at 200-300μCi dose level died within 3-4 weeks following treatment suggesting that these dose levels are associated with increased toxicity (**Appendix-B; Figure-7**).

RIT experiment 5: In this study, the anti-tumor effect of ^{90}Y-DOTA-J591 was compared to that of ^{90}Y-DOTA-J415. Mice with LNCaP tumors (150-400mg) were divided into 3 groups (n=7/group). The control group received no treatment. Group-2 received a total of 3 doses (60μCi/dose) of ^{90}Y-DOTA-J591 over a period of 2 months (day 0, 35, 63). Group-3 received a total of 3 doses (60μCi/dose) of ^{90}Y-DOTA-J415 over a period of 2 months (day 0, 35, 63). Compared to controls, both J591 and J415 radiolabeled MAb preparations had a significant anti-tumor response. The % survival with both antibodies was significantly greater compared to controls. However, there is not much difference between these two antibodies **(Appendix-B; Figure-8).**

RIT experiment 6: In this study, the anti-tumor effect of ^{177}Lu-DOTA-J591 was studied. 3 groups of mice (n = 6-7/group) with LNCaP tumors (100-200 mg) were injected with a single dose of 100, 200, and 400μCi of ^{177}Lu-DOTA-J591. A control group received no treatment. With 100μCi, there was a delay in tumor growth. But at 200-400μCi dose levels, the anti-tumor effect was significant compared to controls. 6-8 weeks following treatment, tumors started growing slowly. Compared to control mice, there was a greater survival rate at 100-200μCi dose levels, but at 400μCi dose appears to be toxic (**Appendix-B; Figure-9A**). There was a gradual reduction (20% within 6-8 weeks) in the total body mass of mice in the control group.
In contrast, mice treated with 200μCi of ^{177}Lu, showed no reduction in the body mass. But at 400μCi dose level, 50% of the mice had a gradual decline in the body mass and died within 3-6 weeks (**Figure-9B**).

Table 1. **Uptake of Radiolabeled mAbs (%ID/g) and Tumor/non/Tumor ratios in Nude Mice Bearing LNCaP Tumors at 1 day post injection**

Organ	^{131}I-B1 (n=4) mean ±stdev	^{131}I-J415 (n=3) mean ±stdev	^{131}I-J591 (n=8) mean ±stdev
Blood	10.10 ± 1.30	11.10 ± 1.9	12.90 ± 2.6
Heart	2.86 ± 0.51	3.39 ± 0.98	4.06 ± 1.07
Lung	4.30 ± 0.20	5.37 ± 1.32	5.25 ± 1.20
Liver	2.17 ± 0.28[ab]	3.31 ± 0.55[a]	4.11 ± 0.92[b]
Kidney	2.29 ± 0.28	2.83 ± 0.50	2.77 ± 0.71
Stomach	1.54 ± 0.31[b]	2.04 ± 0.40	2.82 ± 0.85[b]
Sm. Intestine	1.15 ± 0.05	1.01 ± 0.22	1.14 ± 0.25
Lg. Intestine	0.38 ± 0.07[b]	0.57 ± 0.03	0.93 ± 0.38[b]
Muscle	0.86 ± 0.11	0.74 ± 0.30	. 0.60 ± 0.52
Thyroid	16.70 ± 12.0	7.73 ± 5.31[c]	15.20 ± 1.6[c]
Spleen	--------	3.36 ± 0.46	3.15 ± 0.62
Tumor	4.41 ± 0.80[a]	12.2 ± 3.24[a]	8.55 ± 3.66
T/Blood	0.45 ± 0.14[a]	1.11 ± 0.13[ac]	0.70 ± 0.28[c]
T/Muscle	5.15 ± 0.70[ab]	18.8 ± 8.2[a]	10.60 ± 6.0[b]
T/Liver	2.08 ± 0.54$_a$	3.73 ± 0.58[a]	2.27 ± 1.23
T/Spleen	--------	3.67 ± 0.61[c]	2.45 ± 0.40[c]

Notes:
a: $p<0.05$ for ^{131}I-B1 vs. ^{131}I-J415
b: $p<0.05$ for ^{131}I-B1 vs. ^{131}I-J591
c: $p<0.05$ for ^{131}I-J415 vs. ^{131}I-J591.

Table 2. **Biodistribution of Radiolabeled MAbs (%ID/g) and Tumor to Non/Tumor Ratios in Nude Mice Bearing LNCaP Tumors at 2 days post injection.**

Organ	^{131}I-J415 (n=8) mean±stdev	^{131}I-J533 (n=4) mean±stdev	^{131}I-J591 (n=8) mean±stdev	^{131}I-7E11 (n=7) mean±stdev	^{111}In-J415 (n=4) mean±stdev	^{111}In-J591 (n=4) mean±stdev	^{111}In-7E11 (n=4) mean±stdev
Blood	8.44 ± 2.16[a]	12.80 ± 1.1[ad]	8.57 ± 2.04[d]	10.80 ± 3.5	6.12 ± 0.62[gh]	8.98 ± 2.10[g]	7.22 ± 0.46[h]
Heart	2.71 ± 0.66[ac]	4.82 ± 1.47[ad]	2.78 ± 0.62[df]	3.92 ± 0.99[cf]	2.87 ± 0.44	3.10 ± 0.36	2.72 ± 0.81
Lung	4.38 ± 0.92	5.08 ± 0.45	4.65 ± 1.77	4.68 ± 0.54	4.15 ± 0.99[gh]	5.89 ± 0.30[gi]	4.64 ± 0.27[hi]
Liver	2.56 ± 0.63[a]	3.78 ± 0.50[ade]	2.71 ± 0.50[d]	2.96 ± 0.52[e]	5.18 ± 1.07[gh]	7.68 ± 0.50[gi]	4.49 ± 0.51[hi]
Kidney	2.05 ± 0.41[b]	3.37 ± 0.39[de]	2.11 ± 0.57[bd]	2.16 ± 0.88[e]	4.21 ± 0.07[gh]	5.25 ± 0.63[gi]	2.55 ± 0.27[hi]
Stomach	1.37 ± 0.37	1.11 ± 0.34	1.46 ± 0.40	1.17 ± 0.26	1.16 ± 0.29	0.73 ± 0.18	0.92 ± 0.37
Sm Intestine	1.01 ± 0.37	0.84 ± 0.07	0.86 ± 0.18	0.94 ± 0.09	1.39 ± 0.06	1.32 ± 0.26[i]	1.06 ± 0.19[i]
Lg Intestine	0.50 ± 0.21	0.43 ± 0.13	0.54 ± 0.13[f]	0.39 ± 0.06[f]	0.76 ± 0.13[g]	0.98 ± 0.06[g]	0.70 ± 0.13
Muscle	0.70 ± 0.19[a]	1.13 ± 0.26[ad]	0.62 ± 0.19[df]	0.95 ± 0.24[f]	0.83 ± 0.09	0.67 ± 0.10	0.83 ± 0.37
Thyroid	18.90 ± 5.9[a]	30.20 ± 8.3[ade]	15.70 ± 10.57[df]	19.4 ± 4.1[ef]	2.19 ± 0.72	2.47 ± 0.37[i]	1.67 ± 0.19[i]
Spleen	2.47 ± 0.62	2.60 ± 0.29	2.88 ± 0.89	2.40 ± 0.45	4.48 ± 1.11	5.36 ± 1.25	3.94 ± 1.13
Tumor	13.00 ± 5.1	7.38 ± 0.97[d]	11.20 ± 2.9[d]	11.70 ± 4.3	11.3 ± 1.0[h]	13.6 ± 2.8[i]	9.3 ± 1.52[hi]
T/Blood	1.57 ± 0.42[ac]	0.58 ± 0.04[ade]	1.43 ± 0.57[d]	1.08 ± 0.18[ce]	1.83 ± 0.33	1.62 ± 0.72	1.34 ± 0.24
T/Liver	5.19 ± 1.35[a]	1.96 ± 0.18[ade]	4.37 ± 1.15[d]	3.89 ± 0.92[e]	2.20 ± 0.52	1.76 ± 0.22	2.16 ± 0.44
T/Spleen	5.45 ± 1.69[a]	2.84 ± 0.32[a]	3.85 ± 1.55	3.73 ± 1.55	2.59 ± 0.76	2.39 ± 0.86	2.59 ± 0.92
T/Muscle	19.20 ± 6.0[ac]	6.80 ± 1.56[ade]	20.0 ± 6.9[df]	12.3 ± 2.2[cef]	13.4 ± 1.4	21.10 ± 7.4	13.80 ± 7.8

Notes:

a: $p<0.05$ for ^{131}I-J415 vs. ^{131}I-J533
b: $p<0.05$ for ^{131}I-J415 vs. ^{131}I-J591
c: $p<0.05$ for ^{131}I-J415 vs. ^{131}I-7E11
d: $p<0.05$ for ^{131}I-J533 vs. ^{131}I-J519
e: $p<0.05$ for ^{131}I-J533 vs. ^{131}I-7E11
f: $p<0.05$ for ^{131}I-J591 vs. ^{131}I-7E11
g: $p<0.05$ for ^{111}In-J415 vs. ^{111}In-J519
h: $p<0.05$ for ^{111}In-J415 vs. ^{111}In-7E11
i: $p<0.05$ for ^{111}In-J591 vs. ^{111}In-7E11.

Table 3. **Biodistribution of Radiolabeled MAbs (%ID/g) and Tumor to Non/Tumor Ratios in Nude Mice Bearing LNCaP Tumors at 4 days post injection.**

Organ	^{131}I-J415 (n=9) mean ±stdev	^{131}I-J533 (n=4) mean ±stdev	^{131}I-J591 (n=7) mean ±stdev	^{131}I-7E11 (n=8) mean ±stdev	^{111}In-J415 (n=4) mean ±stdev	^{111}In-J591 (n=7) mean ±stdev	^{111}In-7E11 (n=4) mean ±stdev
Blood	6.11 ±0.97[ac]	10.3 ±0.48[ade]	5.96 ±1.61[d]	7.72 ±1.79[ce]	4.42 ±0.78	4.78 ±0.85	5.69 ±1.00
Heart	2.01 ±0.54[a]	2.87 ±0.71[ad]	1.70 ±0.16[fd]	2.59 ±1.03	1.84 ±0.45	1.82 ±0.37	1.58 ±0.49
Lung	3.51 ±0.85	4.49 ±1.05	3.35 ±0.97	3.80 ±0.76	3.72 ±0.50	3.40 ±0.32	4.03 ±1.03
Liver	1.97 ±0.40[a]	2.56 ±0.18[ae]	2.06 ±0.46	1.93 ±0.33[e]	5.47 ±0.50h	7.66 ±2.44[i]	4.39 ±0.45[hi]
Kidney	1.94 ±0.60[b]	2.27 ±0.55[de]	1.37 ±0.24[bd]	1.66 ±0.33[e]	5.22 ±0.57h	5.39 ±1.27	3.81 ±2.08
Stomach	0.96 ±0.55	0.98 ±0.21	1.06 ±0.36	0.96 ±0.23	1.35 ±0.37[g]	0.80 ±0.15[g]	1.02 ±0.35
Sm Intestine	0.62 ±0.29	0.76 ±0.13[d]	0.53 ±0.13[fd]	0.77 ±0.08	1.69 ±0.19[gh]	1.31 ±0.19[gi]	0.94 ±0.06[hi]
Lg Intestine	0.32 ±0.16[c]	0.31 ±0.04[e]	0.34 ±0.10[f]	0.48 ±0.10[ce]	0.88 ±0.06h	0.81 ±0.20[i]	0.50 ±0.07[hi]
Muscle	0.62 ±0.37	0.93 ±0.28[d]	0.48 ±0.24[d]	0.72 ±0.27	0.60 ±0.03	0.55 ±0.34	0.51 ±0.13
Thyroid	26.6 ±17.9	33.7 ±6.9[e]	26.5 ±26.2	21.3 ±7.9[e]	1.82 ±0.70	1.90 ±0.16[i]	1.29 ±0.69[i]
Spleen	2.43 ±1.04[a]	2.33 ±0.38[a]	2.33 ±0.72	1.99 ±0.69	4.63 ±1.38	4.43 ±0.89	3.88 ±1.51
Tumor	17.0 ±6.6[a]	7.29 ±2.5	11.4 ±4.21	12.1 ±5.3	16.7 ±2.6	15.7 ±3.5	16.2 ±4.29
T/Blood	2.80 ±0.70[ac]	0.72 ±0.29[ad]	2.14 ±0.53[d]	1.58 ±0.79[c]	3.17 ±0.37	3.35 ±0.39	2.83 ±0.51
T/Liver	9.07 ±3.19[a]	2.81 ±0.85[ad]	6.41 ±2.89[d]	6.32 ±3.41	2.32 ±0.16	2.19 ±0.47[i]	3.71 ±1.11[i]
T/Spleen	7.70 ±3.81[a]	3.06 ±0.65[ade]	5.71 ±2.21[d]	5.91 ±1.67[e]	2.50 ±0.11[gh]	3.67 ±0.71[g]	4.32 ±0.85[h]
T/Muscle	30.7 ±11.3[ac]	7.85 ±1.25[ade]	29.9 ±10.3[df]	18.1 ±8.0[ce]	21.8 ±2.4[h]	40.1 ±22.6	32.1 ±4.9[h]

Notes:

a: p<0.05 for ^{131}I-J415 vs. ^{131}I-J533 b: p<0.05 for ^{131}I-J415 vs. ^{131}I-J591 c: p<0.05 for ^{131}I-J415 vs. ^{131}I-7E11

d: p<0.05 for ^{131}I-J533 vs. ^{131}I-J519 e: p<0.05 for ^{131}I-J533 vs. ^{131}I-7E11 f: p<0.05 for ^{131}I-J591 vs. ^{131}I-7E11

g: p<0.05 for ^{111}In-J415 vs. ^{111}In-J519 h: p<0.05 for ^{111}In-J415 vs. ^{111}In-7E11 i: p<0.05 for ^{111}In-J591 vs. ^{111}In-7E11.

Table 4. **Biodistribution of Radiolabeled MAbs (%ID/g) and Tumor to Non/Tumor Ratios in Nude Mice Bearing LNCaP Tumors at 6 days post injection.**

Organ	^{131}I-J415 (n=5) mean ±stdev	^{131}I-J591 (n=8) mean ±stdev	^{131}I-7E11 (n=8) mean ±stdev	^{111}In-J415 (n=4) mean ±stdev	^{111}In-J591 (n=8) mean ±stdev	^{111}In-7E11 (n=4) mean ±stdev
Blood	3.95 ±0.99[b]	4.42 ±1.74[c]	7.13 ±1.90[bc]	2.63 ±0.47[e]	2.52 ±0.56[f]	4.16 ±0.41[ef]
Heart	1.57 ±0.47[b]	1.42 ±0.60[c]	2.46 ±0.46[bc]	1.30 ±0.10	1.28 ±0.24	2.42 ±1.49
Lung	2.61 ±1.00	2.29 ±0.91[c]	3.52 ±0.59[c]	3.07 ±0.67	2.47 ±0.65	3.20 ±0.16
Liver	1.74 ±0.91	1.31 ±0.34[c]	2.01 ±0.49[c]	4.69 ±0.61[d]	6.08 ±0.83[df]	4.37 ±0.46[f]
Kidney	1.36 ±0.62	1.20 ±0.51	1.65 ±0.39	4.67 ±0.45[e]	4.53 ±0.87[f]	2.85 ±0.26[e]
Stomach	0.54 ±0.19	0.47 ±0.15	0.47 ±0.23	0.44 ±0.20	0.46 ±0.17	0.31 ±0.07
Sm Intestine	0.47 ±0.15	0.35 ±0.09[c]	0.52 ±0.14[c]	0.93 ±0.04[e]	0.84 ±0.13[f]	0.64 ±0.08[ef]
Lg Intestine	0.30 ±0.16	0.24 ±0.07[c]	0.38 ±0.12[c]	0.71 ±0.13	0.57 ±0.10	0.64 ±0.06
Muscle	0.30 ±0.06[b]	0.33 ±0.18[c]	0.74 ±0.31[bc]	0.35 ±0.11	0.30 ±0.10	0.36 ±0.08
Thyroid	28.5 ±13.1	35.1 ±18.4	29.3 ±10.6	1.66 ±0.22[de]	0.85 ±0.36[df]	1.38 ±0.25[ef]
Spleen	1.37 ±0.25	1.74 ±0.72	1.74 ±0.38	4.32 ±1.32	3.36 ±0.61	3.14 ±0.60
Tumor	15.4 ±2.4[a]	9.58 ±3.2[ac]	14.5 ±4.8[c]	17.7 ±3.1	17.4 ±3.5	18.7 ±2.2
T/Blood	4.49 ±1.81[ab]	2.28 ±0.77[a]	2.21 ±1.33[b]	6.78 ±0.78[e]	6.07 ±1.79	4.57 ±0.31[e]
T/Liver	11.7 ±5.5	7.21 ±1.80	7.38 ±2.40	3.79 ±0.47[e]	3.22 ±0.52[f]	4.33 ±0.85[ef]
T/Spleen	9.69 ±3.73	6.90 ±2.20	8.89 ±3.84	4.57 ±2.33	5.14 ±0.95	6.52 ±2.32
T/Muscle	56.1 ±11.2[ab]	34.1 ±15.9[a]	21.8 ±12.9[b]	52.1 ±11.2[d]	64.3 ±5.9[d]	55.6 ±12.8

a: $p<0.05$ for ^{131}I-J415 vs. ^{131}I-J591 b: $p<0.05$ for ^{131}I-J415 vs. ^{131}I-7E11 c $p<0.05$ for ^{131}I-J591 vs. ^{131}I-7E11
d: $p<0.05$ for ^{111}In-J415 vs. ^{111}In-J519 e: $p<0.05$ for ^{111}In-J415 vs. ^{111}In-7E11 f: $p<0.05$ for ^{111}In-J591 vs. ^{111}In-7E11.

TABLE 5. **Biodistribution and Tumor Uptake of ^{177}Lu-DOTA-J591: Comparison with ^{111}In-DOTA-J591.**

	% Injected Dose/g with					
	^{177}Lu-DOTA-J591			^{111}In-DOTA-J591		
Organ	Day 1	Day 2	Day 4	Day1	Day 2	Day 4
Tumor (T)	11.2 ± 0.7	15.9 ± 1.7	19.3 ± 4.3	10.2 ± 0.7	13.6 ± 1.4	15.7 ± 1.3
Blood (B)	12.2 ± 0.6	8.9 ± 0.4	4.3 ± 0.8	11.1 ± 1.5	9.9 ± 1.1	4.8 ± 0.3
Liver	6.1 ± 0.8	4.7 ± 0.4	4.1 ± 0.4	8.9 ± 0.7	7.7 ± 0.3	7.7 ± 0.9
Kidney	5.1 ± 0.8	4.1 ± 0.2	3.3 ± 0.2	7.7 ± 0.5	5.3 ± 0.3	5.4 ± 0.5
Spleen	2.6 ± 0.5	3.3 ±0.2	3.3 ± 0.6	4.8 ± 0.4	5.4 ± 0.6	4.4 ± 0.3
Muscle(M)	0.75 ± 0.04	0.65 ± 0.02	0.77 ± 0.29	1.37 ± 0.29	0.67 ± 0.05	0.55 ± 0.13
T/B	0.92	1.8	4.5	0.92	1.4	3.3
T/M	14.9	24.5	25.0	7.5	20.3	28.5

TABLE 6: RIT of Prostate Cancer: Studies in nude mice with LNCaP tumors

RIT expt.#.	Group-1	Group-2	Group-3	Group-4	Group-5
1.	**Control:** (untreated)	^{131}I-J591(100μCi)	^{131}I-J591 (100μCi, ip)	^{131}I-J591 (300μCi)	
2.	**Control:** (untreated)	^{131}I-J591(300μCi)	^{90}Y-DOTA-J591 (35μCi)	^{90}Y-DOTA-J591 (35μCi) (2 doses)	
3.	**Control**: (untreated)	^{90}Y-DOTA-F23 (30μCi) (**Control**: non-specific MAb)	^{90}Y-DOTA-J591 (30μCi) (3 doses)	^{90}Y-DOTA-J591 (60μCi) (3 doses)	^{90}Y-DOTA-J591 (90μCi) (3 doses)
4.	**No cotrol**	^{90}Y-DOTA-J591 (150μCi)	^{90}Y-DOTA-J591 (200μCi)	^{90}Y-DOTA-J591 (300μCi)	
5.	**Control:** (untreated)	^{90}Y-DOTA-J591 (60μCi) (3 doses)	^{90}Y-DOTA-J415(60μCi) (3 doses)		
6.	**Control:** (untreated)	^{177}Lu-DOTA-J591(100μCi)	^{177}Lu-DOTA-J591 (200μCi)	^{177}Lu-DOTA-J591 (400μCi)	

For RIT studies, radiolabeled antibody dose was injected in the **tail vein**; only in one group (experiment 1 group-3, dose was given intraperitoneally)
In some studies, the mice received 2 or 3 repeated dose injections over a period of 2 months

KEY RESEARCH ACCOMPLISHMENTS:

1. We have optimized the techniques of radiolabeling MAbs with ^{131}I, ^{111}In, ^{90}Y, and ^{177}Lu in order to achieve high specific activities (5-10mCi/mg) with out significant loss of immunoreactivity.

2. We have clearly demonstrated that MAbs J591, J415 and J533 bind specifically to the extracellular domain of $PSMA_{ext}$. We have also identified that J591 and J415 compete for binding to PSMA, while J533 competes with J591 but not J415. In addition, we have clearly documented that 7E-11 MAb (specific to intracellular portion of PSMA) does not inhibit the binding of J591, J415 and J533 to PSMA positive LNCaP tumor cells.

3. In nude mice with LNCaP tumors, we demonstrated that the tumor uptake of radiolabeled J591 and J415 is very specific. The absolute tumor uptake and tumor/blood ratios are much greater with ^{111}In or ^{177}Lu labeled antibodies compared to ^{131}I labeled antibodies.

4. In nude mice with LNCaP tumors, we have demonstrated that the anti-tumor effect of ^{131}I-J591, ^{90}Y-DOTA-J591 and ^{177}Lu-DOTA-J591 MAbs is dependent on the dose of radionuclide administered. 60-90μCi of ^{90}Y and 200μCi of ^{177}Lu labeled J591 have a significant anti-tumor response with minimal toxicity. We have also demonstrated that the anti-tumor effect of radiolabeled J591 is specific since ^{90}Y-labeled non-specific antibody did not have any anti-tumor effect.

5. We have identified that both J415 and J591 are promising MAbs for the targeting of viable PSMA-expressing tumor tissue. ^{111}In-DOTA-J591 (or J415) is potentially useful for non-invasive imaging (radioimmunodiagnosis) of tumor tissue . ^{90}Y-DOTA-J591 and ^{177}Lu-DOTA-J591 MAbs may have significant potential for radioimmunotherapy of prostate cancer.

6. Based on this Phase I research data, we applied for Phase II of the Idea Development of the PCRP. In July 2000, we were awarded funding for the Phase II research proposal to perform a dose escalation trial with ^{90}Y-DOPTA-J591 in patients with prostate cancer.

REPORTABLE OUTCOMES:

1. Vallabhajosula S. Kostakoglu L. Goldsmith S.J. Bastidas D, Navarro V Gomez D. Bander NH. Monoclonal antibody J591 specific to the extracellular domain of PSMA: A new agent for radioimmunodiagnosis (RID) and radioimmunotherapy. J Nucl Med 1998;39(5 Suppl):77P-78P (Abstract).
2. Smith-Jones PM, Vallabhajosula S, Hunter CJ, et al. Monoclonal Antibodies (MAb) specific to extracellular Domain of PSMA: in vitro studies. J Nucl Med 1999; 40: (5suppl): 226p (abstract).
3. Smith-Jones PM, Vallabhajosula S, Bastidas D, et al. In vivo evaluation of I-131 labeled MAbs specific for extracellular Domain of PSMA. J Nucl Med 1999; 40: (5suppl): 225p (abstract).
4. Vallabhajosula S, Smith-Jones PM, Bastidas D, et al. Preclinical studies of radiolabeled J591 MAb specific for extracellular domain of PSMA: Comparison with ProstaScint. Eur J Nucl Med 1999; 26(9):1212 (Abstract).
5. Smith-Jones PM, Vallabhajosula S, Bastidas D, et al. Preclinical studies with ^{131}I and ^{111}In labeled MAbs, specific for the intracellular or extracellular domains of PSMA. J Label Comp Radiopharma 1999; 42:suppl 1,s701-703 (Abstract).
6. Smith-Jones PM, Navarro V, Bander N, Goldsmith SJ, Vallabhajosula S. Uptake and Metabolism of ^{111}In and ^{131}I labeled Anti-PSMA Monoclonal Antibodies by Prostate Carcinoma cells. J. Nucl Med 2000;41:(5 suppl):142p (Abstract).
7. Smith-Jones PM, Vallabhajosula S, Navarro V, Goldsmith SJ, Bander NH. ^{90}Y-huj591 MAb specific to PSMA: Radioimmunotherapy (RIT) studies in nude mice with prostate cancer LNCaP tumor. Eur J Nucl Med 2000; 27(8):951 (Abstract).
8. Smith-Jones PM, Vallabhajosula S, Goldsmith SJ, Navarro V, Hunter CJ, Bastidas D, Bander NH. In vitro Characterization of Radiolabeled Monoclonal Antibodies Specific for the Extracellular Domain of Prostate-specific Membrane Antigen. Cancer Res 2000; 60:5237-5243.

CONCLUSIONS:

1. The MAbs J591, J415 and J533, specific to the extracellular domain of PSMA were all radiolabeled with I-131, In-111, Y-90, and Lu-177 without any significant loss of immunoreactivity. Both in vitro and in vivo studies clearly demonstrated that these MAbs bind specifically to extracellular epitopes of PSMA and do not cross-react with the intracellular epitope that binds specifically 7E11 MAb (ProstaScint). J415 and J591 bind to the same epitope of the extracellular domain of PSMA while J533 binds to a different epitope.

2. The biodistribution studies in nude mice with LNCaP tumors clearly demonstrated that the specific tumor uptake of radiolabeled J591 and J415. There were significant differences in tumor uptake among the ^{131}I MAbs. By contrast, the tumor uptake of ^{111}In labeled MAbs was similar. The absolute tumor uptake of ^{177}Lu-DOTA-J591 was slightly higher than that of ^{111}In-DOTA-J591. The T/B and T/M are higher with ^{111}In and ^{177}Lu compared to that of ^{131}I labeled J591 MAb.

3. The kinetics of wash out and the net cell retention of ^{131}I and ^{111}In labeled MAbs was significantly different. The net retention with ^{111}In (70-80%) was much greater than with ^{131}I (30%).

4. In nude mice with LNCaP tumors, ^{131}I-J591, ^{90}Y-DOTA-J591, and ^{177}Lu-DOTA-J591 produced an unambiguous dose-response resulting in tumor shrinkage or slowing the growth over a period of 4-6 weeks. The most important finding is that this therapeutic response was specific since ^{90}Y-non-specific MAb had no response. The anti-tumor effect of ^{177}Lu-DOTA-J591 (at 200μCi dose level) appears to be similar to that with ^{90}Y-DOTA-J591 (at 60μCi dose level). But the toxicity with ^{177}Lu appears to be less compared to that with ^{90}Y and ^{131}I.

5. These results clearly demonstrate that radiolabeled MAbs specific to the external domain of PSMA are useful for RID and RIT of prostate cancer.

REFERENCES

1. Israeli R.S., Powell C.T., Corr J.G., Fair W.R., and Heston W.D.W.. Expression Of The Prostate-Specific Membrane Antigen. Cancer Res 1994; 54: 1807-1811
2. Kahn D., Williams R.D., Seldin D.W., Linbertino J.A., Hirschhorn M., Dreicer R., Weiner G.J., Bushnell D. and Gulfo J.. Radioimmunoscintigraphy With ^{111}Indium Labeled CYT-356 For The Detection Of Occult Prostate Cancer Recurrence. J. Urol 1994; 152: 1490-1495.
3. Troyer J.K., Feng Q., Beckett M.L., and Wright G.L.Jr.. Biochemical Characterization and Mapping of the 7E11-C5.3 Epitope of the Prostate-Specific Membrane Antigen. Urol. Oncol 1995;1: 29-37.
4. Wright G.L., Grob B.M., Haley C., Grossman K., Newhall K., Petrylak D., Troyer J., Konchuba A., Schellhammer P.F. and Moriarty R.. Upregulation Of Prostate Specific Membrane Antigen After Androgen-Depravation Therapy. Urology 1996; *48:* 326-334.
5. Silver D.A., Pellicer I., Fair W.R., Heston W.D.W. and Cordon-Cardo C.. Prostate Specific Membrane Antigen Expression In Normal And Malignant Human Tissues. Clin. Cancer Res 1997; 3: 81-85.
6. Sweat S.D., Pacelli A., Murphy G.P., and Bostwick D.G. Prostate-Specific Membrane Antigen Expression Is Greatest In Prostate Adenocarcinoma And Lymph Node Metastases. Urology 1998; *52:* 637-640.
7. Sweat S.D., Pacelli A., Murphy G.P. and Bostwick D.G. Prostate-Specific Membrane Antigen Expression Is Greatest In Prostate Adenocarcinoma And Lymph Node Metastases. Urology 1998; 52: 637-40.
8. Murphy G.P., Elgamal A.A., Su S.L., Bostwick D.G., and Holmes E.H. Current Evaluation Of The Tissue Localization And Diagnostic Utility Of Prostate Specific Membrane Antigen. Cancer 1998; 83: 2259-2269.
9. Murphy G.P., Elgamal A.A., Su S.L., Bostwick D.G., and Holmes E.H. Current Evaluation Of The Tissue Localization And Diagnostic Utility Of Prostate Specific Membrane Antigen. Cancer 1998; *83:* 2259-2269.

10. Gregorakis A.K., Holmes E.H. and Murphy G.P.. Prostate-Specific Membrane Antigen; Current and Future Utility. Sem. Urol. Oncol 1998; 16: 2-12.

11. Lui H., Moy P., Kim S., Xia Y., Rajasekaran A., Navarro V., Knudsen B. and Bander N.H. Monoclonal Antibodies To The Extracellular Domain Of Prostate Specific Membrane Antigen Also React With Tumor Vascular Endothelium. Cancer Res 1997; *57:* 3629-3634.

12. Lui H., Rajasekaran A.K., Moy P., Xia Y., Kim S., Navarro V., Rahmati R., and Bander N.H. Constitutive And Antibody-Induced Internalization Of Prostate Specific Membrane Antigen. Cancer Res 1998; *58:* 4055-4060.

13. Chang S.S., Reuter V.E., Heston W.D., Bander N.H., Grauer L.S., and Gaudin P.B. Five different anti-prostate-specific membrane antigen (PSMA) antibodies confirm PSMA expression in tumor-associated neovasculature. Cancer Res 199; *59:* 3192-3198.

14. Chang S.S., O'Keefe D.S., Bacich D.J., Reuter V.E., Heston W.D.W. and Gaudin P.B.. Prostate specific Membrane Antigen Is Produced in Tumor-associated Neovasculature. Clin. Cancer Res 1999; 5: 2674-2681.

15. Petronis J.D., Regan F., and Lin K.. Indium-111 Capromab Pendetide (Prostascint) Imaging To Detect Recurrent And Metastatic Prostate Cancer. Clin. Nucl. Med 1998; *23:* 672-677.

16. Deb N., Goris M., Trisler K., Fowler S., Saal J., Ning S., Becker M., Marquez C., and Knox S. Treatment Of Hormone-Refractory Prostate Cancer With ^{90}Y-CYT-356 Monoclonal Antibody. Clin. Cancer Res 1996; *2:* 1289-1297.

17. Fraker P.J., and Speck J.C. Protein And Cell Membrane Iodinations With A Sparingly Soluble Chloramide, 1,3,4,6-Tetrachloro-3a,6a-Diphenylglycoluril. Biochem. Biophys. Res. Commun 1978; *80:* 849-857.

18. Lindmo T., Boven E., Cuttitta F., Fedorko J., and Bunn P.A. Determination Of The Immunoreactive Fraction Of Radiolabeled Monoclonal Antibodies By Linear Extrapolation To Binding At Infinite Antigen Excess. J. Immunol. Methods 1994; *72:* 77-89.

19. Locin M.F, Desreux J.F. and Merciny E.. Coordination of Lanthanides by two Polyamino Polycarboxylic Macrocycles: Formation of Highly Stable Lanthanide Complexes. Inorg. Chem 1986; 25: 2646-2648.

20. Clarke E.T. and Martel A.E.. Stabilities Of Trivalent Metal Ion Complexes Of The Tetraacetate Derivatives Of 12-, 13- And 14-Membered Tertaazamacrocycles. Inorganica Chimica Acta 1991; 190: 37-46.

21. Broan C.J., Cox J.P.L., Craig A.S., Kataky R., Parker D., Harrison A., Randall A.M. and Ferguson G.. Structure and Solution Stability of Indium and Gallium Complexes of 1,4,7-Triazacyclononanetriacetate and of Yttrium Complexes of 1,4,7,10-Tetraazacyclododecanetetraacetate and Related Ligands: Kinetically Stable Complexes for Use in Imaging and Radiotherapy. X-Ray Molecular Structure of the Indium and Gallium Complexes of 1,4,7- Triazacyclononane-1,4,7-triacetic Acid. J. Chem. Soc. Perkin Trans. 1991; 2, 87-99.

22. Smith-Jones P.M., Vallabahajosula S., Goldsmith S. J., Navarro V., Hunter C. J., Bastidas D and Bander N.H.. In Vitro Characterization of Radiolabeled Monoclonal Antibodies Specific for the Extracellular Domain of Prostate Specific Membrane Antigen. Cancer Res 2000; 60: 5237-43.

APPENDIX- A

[CANCER RESEARCH 60, 5237–5243, September 15, 2000]

In Vitro Characterization of Radiolabeled Monoclonal Antibodies Specific for the Extracellular Domain of Prostate-specific Membrane Antigen[1]

Peter M. Smith-Jones,[2] Shankar Vallabahajosula, Stanley J. Goldsmith, Vincent Navarro, Catherine J. Hunter, Diego Bastidas, and Neil H. Bander

Division of Nuclear Medicine, Department of Radiology [P. M. S-J., S. V., S. J. G., C. J. H., D. B.], and Laboratory of Urological Oncology, Department of Urology [V. N., N. H. B.], New York Presbyterian Hospital-Weill Medical College of Cornell University, New York, New York 10021

ABSTRACT

Prostate-specific membrane antigen (PSMA) is a well-characterized cell surface antigen expressed by virtually all prostate cancers (PCas). PSMA has been successfully targeted *in vivo* with ^{111}In-labeled 7E11 monoclonal antibody (mAb; ProstaScint; Cytogen, Princeton, NJ), which binds to an intracellular epitope of PSMA. This work reports the *in vitro* characterization of three recently developed mAbs that bind the extracellular domain of PSMA ($PSMA_{ext}$). Murine mAbs J415, J533, J591, and 7E11 were radiolabeled with ^{131}I and evaluated in competitive and saturation binding studies with substrates derived from LNCaP cells. J415 and J591 were conjugated to 1,4,7,10-tetraazacyclododecane-*N,N′,N″,N‴*-tetraacetic acid labeled with ^{111}In. The uptake and cellular processing of these antibodies were evaluated in viable LNCaP cells. All four mAbs could be labeled with ^{131}I up to a specific activity of 350 MBq/mg with no or little apparent loss of immunoreactivity. Competition assays revealed that J415 and J591 compete for binding to $PSMA_{ext}$ antigen. J533 bound to a region close to the J591 binding epitope, but J533 did not interfere with J415 binding to PSMA. mAb 7E11 did not inhibit the binding of J415, J533, or J591 (or *vice versa*), consistent with earlier work that these latter mAbs bind $PSMA_{ext}$ whereas 7E11 binds the intracellular domain of PSMA. Saturation binding studies demonstrated that J415 and J591 bound with a similar affinity (K_ds 1.76 and 1.83 nM), whereas J533 had a lower affinity (K_d, 18 nM). In parallel studies, all four mAbs bound to a similar number of PSMA sites expressed by permeabilized cells (1,000,000–1,300,000 sites/cell). In parallel studies performed with viable LNCaP cells, J415, J533, and J591 bound to a similar number of PSMA sites (*i.e.,* 600,000–800,000 sites/cell), whereas 7E11 bound only to a subpopulation of the available PSMA sites (95,000 sites/cell). This apparent binding of 7E11 to viable cells can be accounted for by a 5–7% subpopulation of permeabilized cells produced when the cells were trypsinized and suspended. Up to five DOTA chelates could be bound to either J415 or J591 without compromising immunoreactivity. A comparison of the cellular uptake and metabolic processing of the ^{131}I- and ^{111}In-labeled antibodies showed a rapid elimination of ^{131}I from the cell and a high retention of ^{111}In. All four mAbs recognized and bound to similar numbers of PSMAs expressed by ruptured LNCaP cells (*i.e.,* the exposed intracellular and extracellular domains of PSMA). By comparison to J415 and J591, J533 had a lower binding affinity. Both J415 and J591 recognized and bound to the same high number of PSMAs expressed by intact LNCaP. By contrast, 7E11 bound to fewer sites expressed by intact LNCaP cells (*i.e.,* the exposed extracellular domain of PSMA). Both J415 and J591 are promising mAbs for the targeting of viable PSMA-expressing tissue with diagnostic and therapeutic metallic radionuclides.

INTRODUCTION

PCa[3] is the most frequently diagnosed cancer and the second most common cause of cancer mortality in United States males (1). Many groups have studied mAbs for *in vivo* diagnosis and therapy of PCa (3–8), but the only successful application to date has been the targeting of PSMA for *in vivo* imaging. PSMA is a type II membrane protein that is expressed by virtually all PCas (9, 10). Unlike other prostate-related antigens, such as prostate-specific antigen, prostatic acid phosphatase, and prostate secretory protein, PSMA is an integral membrane protein, and therefore, it is not appreciably released into the circulation. PSMA expression has been shown to be up-regulated in both poorly differentiated (11), advanced PCas (9) and after androgen-deprivation therapy (12). Interestingly, PSMA is expressed on the tumor vascular endothelium of other carcinomas and sarcomas (13, 14) but not on normal vascular endothelium, making it also potentially useful as an antibody-mediated diagnostic and therapeutic target across the full spectrum of solid tumors.

Currently, an ^{111}In-labeled form of the 7E11 murine mAb is approved by the Food and Drug Administration (Prostascint) for the clinical detection of recurrent and metastatic prostate cancer in soft tissue (15). 7E11 mAb binds to the intracellular portion (NH_2 terminus) of the PSMA antigen and, as such, does not bind viable cells (13, 14). It is believed that successful imaging with Prostascint results from mAb binding to antigen exposed in dead or dying cells within some tumor sites (16, 17). Early clinical trials using ^{90}Y-labeled 7E11 resulted in no objective or biochemical (prostate-specific antigen) remissions (7).

Recently, a series of mAbs to $PSMA_{ext}$ has been characterized and reported (13, 14, 18). In this current study, we report on the *in vitro* evaluation of radiolabeled forms of these antibodies against $PSMA_{ext}$ and the selection of interesting candidates for *in vivo* evaluation of their diagnostic and therapeutic potential.

MATERIALS AND METHODS

Murine mAbs J415, J533, and J591 were produced as described earlier (13). Purified 7E11 was generously provided by Dr. Gerald P. Murphy (Pacific Northwest Research Foundation, Seattle, WA). ^{131}I and ^{111}In were purchased from Norton International (Kanata, Ontario, Canada). ^{90}Y was purchased from New England Nuclear (Boston, MA). DOTA was purchased from Macrocyclics, Inc. (Richardson, TX).

LNCaP cells (American Type Culture Collection, Rockville, MD) were grown in RPMI 1640, supplemented with 10% FCS, at a temperature of 37°C in an environment containing 5% CO_2. Prior to use, the cells were trypsinized, counted, and suspended in serum-free medium. LNCaP cells were permeabilized by adding methanol at −80°C to the cells. The cells were maintained at −20°C for 20 min before the methanol was removed, and the cells were rehydrated by washing four times with PBS (with 5 mM Ca^{2+} and 5 mM Mg^{2+}) over 20 min.

Cell membranes were prepared by lysing the cells with a Polytron in a

Received 5/3/00; accepted 7/17/00.

The costs of publication of this article were defrayed in part by the payment of page charges. This article must therefore be hereby marked *advertisement* in accordance with 18 U.S.C. Section 1734 solely to indicate this fact.

[1] This work was supported by Grant PC970229 from the United States Department of Army and grants from Yablans Research Fund and CaP Cure. N. H. B. is a consultant to BZL Biologics, Inc. The agreement that N. H. B. has with BZL is managed by Cornell University in accordance with its conflict of interest policies.

[2] To whom requests for reprints should be addressed, at Weill Medical College of Cornell University, 525 East 68th Street, Starr 221, New York, NY 10021. E-mail: psj2001@med.cornell.edu.

[3] The abbreviations used are: PCa, prostate cancer; mAb, monoclonal antibody; PSMA, prostate-specific membrane antigen; DOTA, 1,4,7,10-tetraazacyclododecane-*N,N′,N″,N‴*-tetraacetic acid; BSA, bovine serum albumin; TLC, instant TLC; HPLC, high-performance liquid chromatography; DTPA, diethylenetriaminepentaacetic acid.

hypotonic buffer [1 mM Na_2CO_3 (pH 7.4) with 1 mM EDTA and 1 mM phenylmethylsulfonyl fluoride). Large fragments were removed by centrifuging at 2000 × *g*. The supernatant was centrifuged at 150,000 × *g* for 2 h, and the pelleted membranes were resuspended in PBS, aliquoted, and frozen at −70°C until required.

Radioiodination

The four murine mAbs were radiolabeled with ^{131}I using the Iodogen (1,3,4,6-tetrachloro-3a,6a-diphenylglycoluril) method (19). Briefly, 10-ml glass tubes were coated with 50 μg of Iodogen by adding 100 μl of a 0.5 mg/ml solution of Iodogen (Pierce, Rockford, IL) in chloroform. The chloroform was removed by blowing a gentle stream of sterile nitrogen into the tube for 30 min before the tubes were sealed and stored in the dark. The iodination reaction was initiated by adding between 4 and 40 MBq of ^{131}I (0.01 M NaOH) to 0.08 mg of mAb in 0.1 ml of ice-cold PBS. This reaction mixture was allowed to react for 5 min on ice before being loaded onto a 10-ml Biogel-P6 column (Bio-Rad Laboratories, Hercules, CA) equilibrated with 1% BSA in PBS. Once the reaction mixture was loaded onto the column, it was washed with 2 ml of 1% BSA PBS before the main ^{131}I-labeled mAb fraction was eluted with 2 ml of 1% BSA PBS. The amount of free iodine in the ^{131}I-labeled mAb preparations was evaluated using instant TLC with a silica gel impregnated glass fiber support and a mobile phase of isotonic saline. Briefly, a portion of the ^{131}I-labeled mAb was spotted on a 10-cm ITLC-SG strip (Gelman Sciences, Ann Arbor, MI) and developed in isotonic saline. Once the solvent front had reached the end of the strip, it was removed from the solvent and cut at an R_f of 0.5. The two portions were assayed for radioactivity, and the radiochemical purity determined using the following equation: radiochemical purity = activity between R_f 0 and 0.5/total activity in strip.

Antibody Conjugation

J415 and J591 antibodies were modified with DOTA by an analogous method to that used by Lewis *et al.* (20). This method uses the direct coupling of one of the four carboxylic acid groups of DOTA to the primary amines present in the protein structure (Fig. 1). Twenty-five mg of antibody were concentrated in a M_r 30,000 Microsep centrifugal concentrator (Pall Filtron, Northborough, MA) and washed with 5 × 4 ml of 1% DTPA (pH 5.0) over a period of 24 h. The antibody buffer was then changed to 0.1 M phosphate (pH 7.0) using the same centrifugal technique. An active ester of DOTA was created by dissolving 146 mg of DOTA (0.361 mmol) and 36 mg of *N*-hydroxysuccinimide (0.313 mmol) in 2 ml of water and adjusting the pH to 7.3 with NaOH, prior to the addition of 10 mg of 1-ethyl-3-(3-dimethylaminopropyl)carbodiimide. This reaction mixture was cooled on ice for 1 h before being added to the J591 solution. The resultant DOTA-antibody conjugate was separated from the excess DOTA and other reactants by repeated washing with 0.3 M NH_4OAc (20 × 4 ml) and centrifugal concentration.

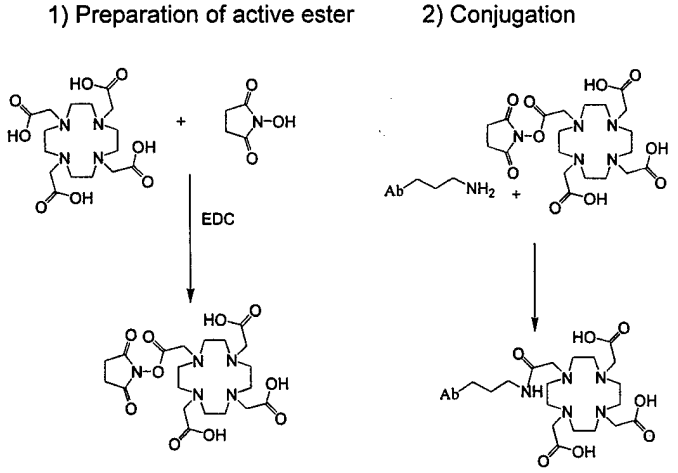

Fig. 1. Two-step conjugation of DOTA to free amines displayed by either J415 or J591. The first step used *N*-hydroxysuccinimide and 1-ethyl-3-(3-dimethylaminopropyl)carbodiimine to create an active ester with DOTA. In the second step, the unpurified active ester is allowed to react with the monoclonal antibody.

Assay of Binding Site Number

DOTA-J591 conjugate concentration was assayed by determining the UV absorption at 280 nm. Two 50-μl aliquots of DOTA-J591 were mixed with either 20 or 40 μl of a 1.30 mM solution of $InCl_3$ (0.01 M HCl) spiked with a tracer amount of ^{111}In. The mixture was incubated at 37°C for 16 h and then analyzed by ITLC, using a silica gel-impregnated glass fiber 10-cm strip (ITLC-SG; Gelman) and an eluant of 1% DTPA (pH 6.0). Antibody-bound activity remains at the origin, and free In^{3+} moves with the solvent front as an $[In\text{-}DTPA]^{2-}$ complex. The relative amounts of In^{3+} and In-DOTA-J591 were determined by cutting the ITLC strip at a R_f of 0.5 and counting the two halves with a Na(Tl)I detector. The number of binding sites was calculated by considering the molar reaction ratio between In and DOTA-mu-J591, and the observed ratio of ^{111}In and ^{111}In-DOTA-mu-J591 was detected.

^{111}In and ^{90}Y Labeling of DOTA Conjugate

Radiolabeling of DOTA-J591 with ^{111}In was achieved by adding the radionuclide (in dilute HCl) to the ammonium acetate-buffered DOTA-J591. Briefly, a mixture composed of 20 μl of $^{111}InCl_3$ (300 MBq), 0.01 M HCl, and 400 μl of DOTA-J591 (4 mg/ml; 0.3 M NH_4OAc, pH 7) was allowed to react at 37°C for 20 min. The reaction mixture was then separated on a 20-ml Biogel-P6 column equilibrated with 4 × 10 ml of sterile 1% HSA in PBS. After the reaction mixture was loaded onto the column, it was washed with an additional 5 ml of 1% HSA PBS before the main ^{111}In-DOTA-J591 fraction was eluted with 3 ml of 1% HSA PBS. A similar procedure was used for radiolabeling with ^{90}Y, but an incubation time of 5 min was used, and the labeling mixture included 50 mM ascorbic acid.

Free ^{111}In in the radiolabeled DOTA-J591 preparations was determined using the ITLC method with a silica gel-impregnated glass fiber support and a mobile phase of 1% DTPA (pH 5.5). A portion of the radiolabeled DOTA-J591 was spotted on a 10-cm ITLC-SG strip and developed in 1% DTPA (pH 5.5). Once the solvent front had reached the end of the strip, it was removed from the solvent and cut at a R_f of 0.5. The two portions were assayed for radioactivity, and the radiochemical purity was determined using the equation described earlier.

Chelate Stability Studies

^{111}In-labeled DOTA-J591 and DTPA-7E11 were mixed with an equal volume of 50 mM DTPA and maintained at 37°C. Periodically, samples were removed and spotted on a 10-cm ITLC-SG strip and developed in 0.9% NaCl. Once the solvent front had reached the end of the strip, it was removed from the solvent and cut at a R_f of 0.5. The two portions were assayed for radioactivity, and the amount of intact chelate was determined using the equation described earlier.

Binding Studies

Immunoreactivity. The immunoreactivity of the ^{131}I- and ^{111}In-labeled mAb preparations was assessed by the method of Lindmo *et al.* (21), which extrapolates the binding of the radiolabeled antibody at an infinite excess antigen. Briefly, six test solutions were prepared (in duplicate) and contained 20,000 cpm of the radioiodinated antibody, and increasing amounts of membranes were prepared from LNCaP cells in a total test volume of 250 μl of PBS (0.2% BSA, pH 7.4). The solutions were incubated at 37°C for 45 min prior to being filtered through a glass membrane filter and washed with ice-cold 10 mM Tris-0.9% NaCl buffer. Filters were counted in a gamma counter with standards representing the total radioactivity added. Data were then plotted as the reciprocal of the substrate concentration (X axis) against the reciprocal of the fraction bound (Y axis). The data were then fitted according to a least squares linear regression method using Origin software (Microcal Software, Inc., Northampton, MA). The Y intercept gave the reciprocal of the immunoreactive fraction. A similar method using intact or permeated LNCaP cells and centrifugational isolation of the cells gave the same results.

Competitive Binding Studies. Competitive binding studies were performed with each of the radioiodinated antibodies and the four unlabeled antibodies using either LNCaP tumor sections or membranes derived from LNCaP tumors. Acetone fixed and frozen 10-μm tumor sections were soaked in Tris buffer [170 mM (pH 7.4), with 2 mM $CaCl_2$ and 5 mM KCl] for 15 min and then washed with Tris buffer (170 mM, pH 7.4). The sections were then

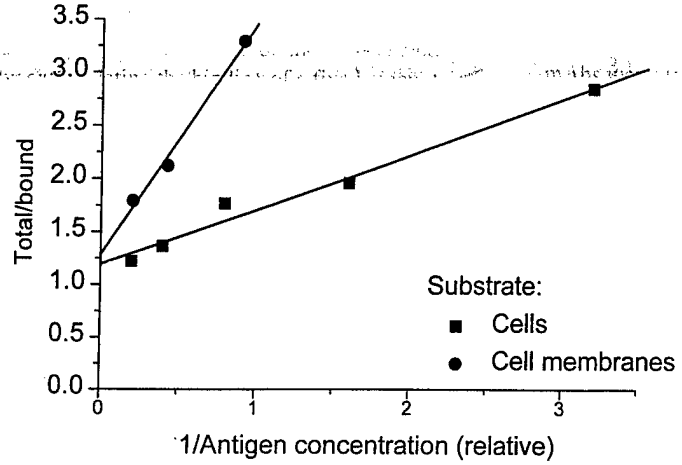

Fig. 2. Lindmo immunoreactivity testing of radiolabeled antibodies. Twenty thousand cpm of radiolabeled antibody is incubated with increasing amounts of LNCaP cell membranes at 37°C for 45 min. The membranes are then isolated by filtration through a glass fiber filter and then counted in a gamma counter. Total/bound data are then plotted as a function of the reciprocal antigen concentration. The *Y* intercept gives the reciprocal of the immunoreactivity. The assay, when performed with either intact LNCaP cells (■) or LNCaP cell membranes (●), gives the same immunoreactivity of ~80% for this labeled mAb.

incubated with the radioiodinated antibodies in the presence of 100 nM concentrations of each of the unmodified mAbs for 1 h at 4°C. Sections were washed three times with PBS (0.2% BSA) and once with Tris buffer (170 mM, pH 7.4) prior to being fixed with acetone and exposed with BioMax film (Kodak). The assay using the membranes typically used 50 μg of membranes, 10 fmol of iodinated antibody, and amounts of competing antibody from 0.25 fmol to 25 pmol in a 250-μl volume of PBS (0.2% BSA). Membranes were isolated as described above, and data were analyzed by a least squares regression method and Origin software (Microcal Software, Inc.) was used to determine the IC_{50}s.

Saturation Binding Studies. Saturation binding studies were performed with each of the radiolabeled antibodies using substrates of intact and permeated LNCaP cells. Briefly, 10 test solutions were prepared (in duplicate) and they contained increasing amounts of the radioiodinated antibodies, 500,000 LNCaP cells in a total volume of 250 μl of PBS (0.2% BSA, pH 7.4). The solutions were incubated at 4°C for 1 h and centrifuged and washed twice with ice-cold PBS (0.2% BSA). For each concentration of radiolabeled antibody, nonspecific binding was determined in the presence of 100 nM of the unmodified antibody. The data were analyzed with a least squares regression method (Origin; Microcal Software, Inc.) to determine the K_d and B_{max} values, and a Scatchard transformation was performed.

Internalization and Cellular Processing of J415 and J591

LNCaP cells were plated in 8-cm^2 Petri dishes and allowed to grow until confluent. One μCi of either the ^{131}I- or ^{111}In-labeled forms of J415, J591, or 7E11 (~0.1–0.2 μg) were added to cells and allowed to incubate for 1 h. The medium was then removed, and the cells were washed once with fresh media. One ml of fresh medium was added, and the cells were incubated for up to 2 days at 37°C. Triplicate samples were periodically removed, and the medium was isolated. Surface bound activity was stripped and collected with an ice-cold acid wash (100 mM acetic acid, 100 mM glycine, pH 3.0). The cells were then treated with 1 ml of a 1% solution of Triton X-100 (containing 5 μg/ml each of antipain, pepstatin, and leupeptin as well as 1 mM phenylmethylsulfonyl fluoride) and kept at on ice for 20 min. The resultant suspension was then centrifuged, and the three samples were counted with a gamma counter. The medium and supernatants were also analyzed by ITLC and size exclusion HPLC to determine the amounts of free iodide produced or the size of the radioactive species created.

RESULTS

Radiolabeling and Quality Control. The radioiodination yield for the four mAbs was typically 70–80%, and the amounts of free iodine in the purified mAbs was <0.3%. Specific activities of 350 MBq/mg were routinely achieved. The immunoreactivities of the ^{131}I-labeled mAbs were determined by extrapolating the binding of a fixed amount of ^{131}I-labeled mAb to an infinite amount of PSMA (Lindmo method; Fig. 2). This method gave immunoreactivities of >75% for all mAbs tested. When labeling conditions were increased to produce specific activities >350 MBq/mg, the immunoreactivity was compromised.

An average of five DOTA molecules could be randomly conjugated to J591 and J415, with little apparent loss of immunoreactivity. Conjugation of an average of eight DOTA molecules to J591 resulted in a 20% reduction in immunoreactivity. A 90% incorporation of ^{111}In could be achieved within 15 min. A 90% incorporation of ^{90}Y could be achieved within 5 min. Using the DOTA-J591 conjugate with an average of five DOTA molecules attached, specific activities of 280 MBq ^{111}In/mg DOTA-J591 and 360 MBq ^{90}Y/mg DOTA-J591 were achieved.

^{111}In-Chelate Stability Studies. A direct comparison of the chelate stability of ^{111}In-DTPA-7E11 and ^{111}In-DOTA-J591 showed that ^{111}In was lost from DTPA-7E11 with an apparent half-life of 11 h, whereas the DOTA chelate had an apparent half-life exceeding 1000 h (Fig. 3).

Competitive Binding Studies: Membranes. Radiolabeled J415 could be displaced from binding to LNCaP cell membranes by both J415 and J591 but not J533 (Fig. 4*A*). The J415 mAb had an mean IC_{50} of 1.5 nM (±0.9; n = 6), and J591 had a mean IC_{50} of 6.6 nM (±4.5; n = 6). Similarly, ^{131}I-labeled J533 could be displaced by J533 and J591 but not by J415 (Fig. 4*B*). In these studies, J533 had a mean IC_{50} of 2.3 nM (±1.5; n = 3), and J591 had a mean IC_{50} of 1.7 nM (±1.3; n = 3). Finally, ^{131}I-labeled J591 could be displaced by J415, J533, and J591 (Fig. 4*C*). The observed IC_{50}s were 1.3 nM (±0.9; n = 6) for J415, 7.7 nM (±5.5; n = 6) for J533, and 3.1 nM (±1.5; n = 6) for J591. The 7E11 mAb did not inhibit the binding of J415, J533, or J591 (or *vice versa*). These data are consistent with earlier data (11) that J415, J533, or J591 bind to the extracellular domain of PSMA, whereas 7E11 binds to the intracellular domain of PSMA (13).

Saturation Binding Studies. The saturation binding curves generated were characteristic of high affinity binding of an antibody to a single class of antigen. These studies, performed with intact LNCaP cells (Fig. 5), demonstrated that J415 and J591 bound with a similar

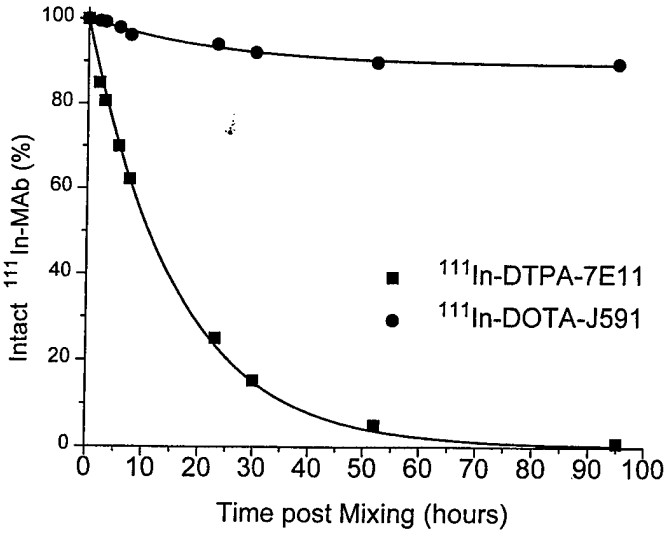

Fig. 3. Stability of ^{111}In-labeled mAbs. The ^{111}In-labeled mAbs were mixed with 50 mM DTPA, and samples were removed and analyzed by ITLC over the next 4 days. ^{111}In-DOTA-J591 (●) had an apparent half-life of >1000 h, and ^{111}In-DTPA-J591 (■) had an apparent half-life of 11 h.

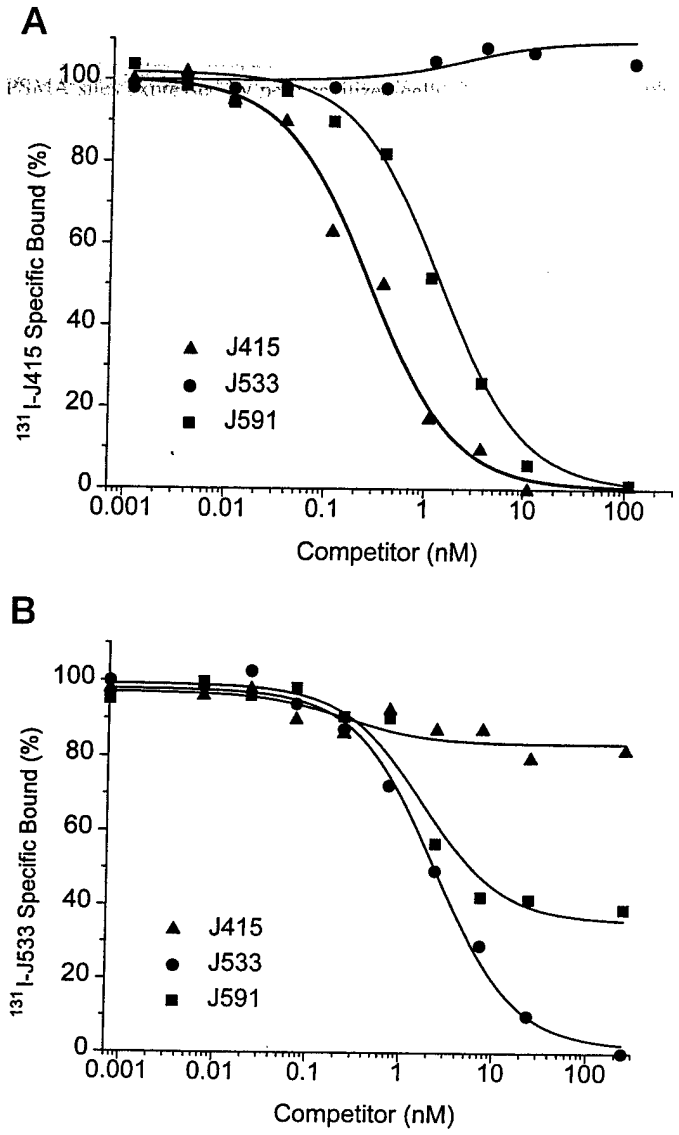

Fig. 4. Displacement binding of ^{131}I-labeled J415 (*A*), ^{131}I-labeled J533 (*B*), and ^{131}I-labeled J591 (*C*) to LNCaP cell membranes. The radioiodinated mAbs are incubated a fixed amount of LNCaP cell membranes in the presence of increasing concentrations of either J415 (▲), J533 (●), or J591 (■) at 37°C for 45 min. The membranes are then isolated by filtration through a glass fiber filter and then counted in a gamma counter. The amount of specific iodinated mAb bound is then plotted as a function of the increasing concentrations of the competing antibodies.

affinity (K_ds 1.76 ± 0.69 and 1.83 ± 1.21 nM), whereas J533 had a lower affinity (K_d 18 ± 5 nM). In parallel studies, all four mAbs bound to a similar number of PSMA sites expressed by permeabilized cells (1,000,000–1,300,000 sites/cell). In parallel studies performed with viable LNCaP cells, J415, J533, and J591 bound to a similar number of PSMA sites (*i.e.*, 600,000–800,000 sites/cell). In contrast, 7E11 specifically bound to only 10–15% of the PSMA sites expressed by apparently intact LNCaP Cells (K_d, 6.69 nM); but when the cells were deliberately ruptured (Fig. 6), 7E11 bound to a similar number of antigen sites as the other three mAbs. In parallel studies, using ^{131}I-labeled J591, permeabilized cells expressed about twice the amount of PSMA as intact LNCaP cells, suggesting that not all available PSMA is simultaneously expressed on the cell surface.

Internalization and Cellular Processing of J415 and J591. Both ^{131}I-labeled J415 and J591 demonstrated a poor cellular retention of

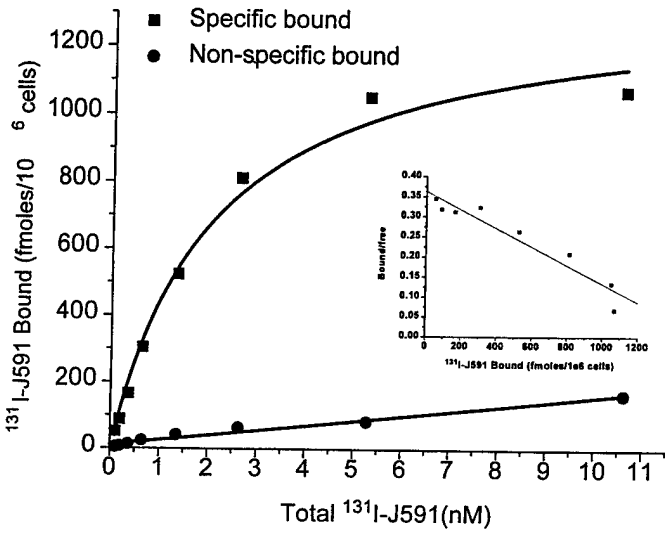

Fig. 5. Saturation binding of ^{131}I-labeled J591 to LNCaP cells. Increasing concentrations of ^{131}I-labeled J591 were incubated with intact LNCaP cells on ice for 60 min. Nonspecific binding (●) was determined in the presence of 100 nM unlabeled J591. Bound activity was isolated by centrifuging the cells and washing them twice with ice-cold buffer. *Inset*, Scatchard plot of the same data.

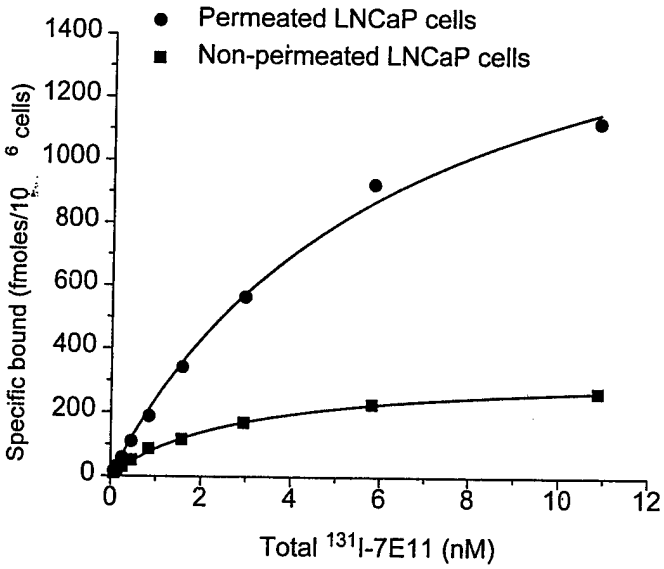

Fig. 6. Saturation binding of ^{131}I-labeled 7E11 to intact and ruptured LNCaP cells. Increasing concentrations of ^{131}I-labeled 7E11 were incubated with either intact (●) or permeabilized (■) LNCaP cells on ice for 60 min. Nonspecific binding was determined in the presence of 100 nM unlabeled 7E11. Bound activity was isolated by centrifuging the cells and washing them twice with ice-cold buffer.

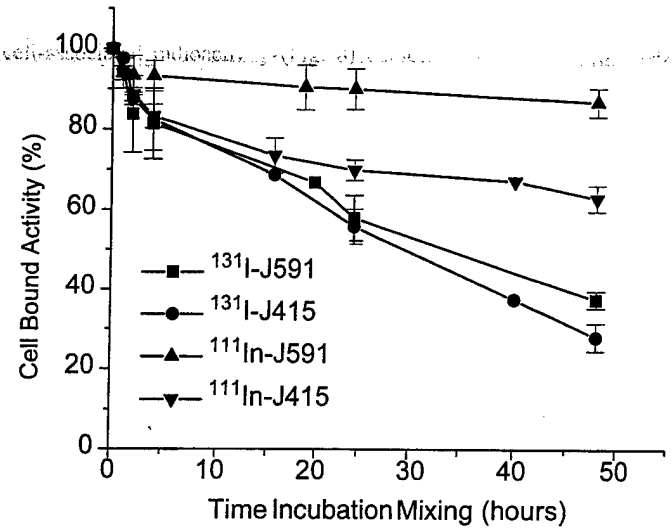

Fig. 7. LNCaP cell retention of radioiodinated J415 and J591. Petri dishes (8 cm^2) with confluent LNCaP cells were incubated with 37 KBq of either ^{131}I-labeled J591 (■), ^{131}I-labeled J415 (●), ^{111}In-labeled J591 (▲), or ^{111}In-labeled J415 (▼). After 1 h at 37°C, the medium was removed, and the cells were washed once with fresh medium. One ml of fresh medium was added, and the cells were incubated for up to 2 days at 37°C. At various time points, the location and form of the radioactivity was determined. *Bars,* SD.

radioactivity (Fig. 7). For both mAbs, a biexponential curve fit of the data showed that ~10% of the radioactivity was released from the cells with an apparent half-life of 1 h, and the remaining 90% was released into the medium with apparent half-lives of 31 and 38 h for J415 and J591, respectively. In parallel studies, ^{131}I-labeled J415 consistently showed a faster release of radioactivity than ^{131}I-labeled J591. Little or no activity (<1%) was associated with the Triton X-100 (or NaOH) insoluble cell pellet. Analysis of the Triton X-100 soluble fractions indicated that there were no appreciable amounts of free ^{131}I present (<1%). HPLC and TLC analysis of the culture medium showed that a large iodinated species, which corresponded to the same size as the intact mAbs, was being released from the cells, but this never amounted to >10% of the total activity, and after 4–6 h, no further release of this radioactive species was observed. The predominant metabolite of the iodinated mAbs found in the cell medium had the same HPLC and TLC elution profile as free $^{131}I^-$. Several studies compared ^{131}I-labeled J591 and DOTA-J591, and no significant differences in the retention of ^{131}I by the cells were noted between the two forms of the same mAb. In all of the studies performed, no increase in cell death was noted as compared with the control groups that received no radiolabeled antibodies.

In comparison to the iodinated mAbs, the ^{111}In-labeled DOTA-J415 and DOTA-J591 demonstrated a high cellular retention of radioactivity (Fig. 7). For ^{111}In-DOTA-J415, a biexponential curve fit of the data showed that ~20% of the radioactivity was released from the cells with an apparent half-life of 2 h, and the remaining 80% was released into the medium with an apparent half-life of 160 h. For ^{111}In-DOTA-J591, the cellular release of ^{111}In species was much slower, and a biexponential curve fit of the data showed that about 5–10% of the radioactivity was released from the cells with an apparent half-life of 1 h, and the remaining 90–95% was being released into the medium with an apparent half-life of 520 h. Little or no activity (<1%) was associated with the Triton X-100 (or NaOH) insoluble cell pellet. HPLC and TLC analysis of the cell medium showed that a large ^{111}In species, which corresponded to the same size at the intact mAbs, was being released from the cells, but this never amounted to >10% of the total activity, and after 4–6 h, no further release of this radioactive species was observed. For both J415 and J591, two main ^{111}In-labeled metabolites were observed in the medium. Analysis of the cell-associated radioactivity (Fig. 8) demonstrated the rapid formation of two groups of metabolites (based on molecular size). One group of metabolites achieved a maximum concentration after 1–2 h, after which it began to steadily decline. The second group of metabolites, however, demonstrated an ever-increasing intracellular concentration. This second metabolite did not behave the same as $^{111}In^{3+}$ (HPLC or TLC), but rather it had a similar molecular weight as an ^{111}In-DOTA or an ^{111}In-DOTA-amino acid fragment. The first metabolite had a molecular weight between that of the intact mAb and the second metabolite (M_r ~10,000–30,000).

The uptake rates of ^{111}In-labeled J415, J591, and 7E11 by LNCaP cells showed a similar initial uptake rate for J415 and J591, which was 10–20 times faster than that of 7E11 (Fig. 9). However, by 4 h after the addition of the radioactivity, the cells treated with ^{111}In-DOTA-J591 have incorporated and retained more activity than those treated with ^{111}In-DOTA-J415.

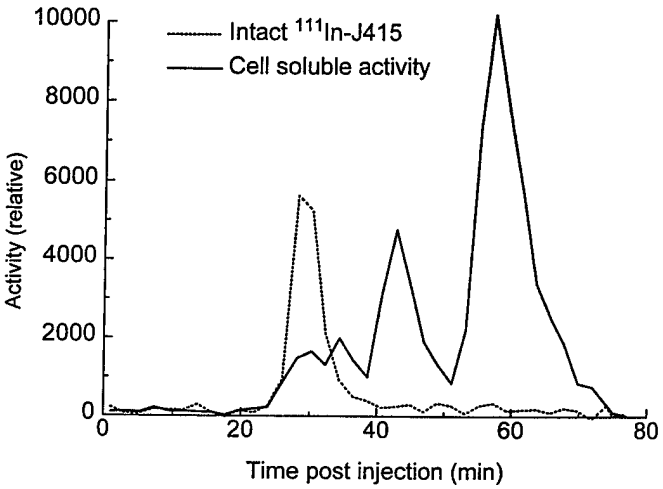

Fig. 8. HPLC chromatograms of ^{111}In-DOTA-J415 and radioactivity recovered from LNCaP cells at 48 h after incubation. The intact ^{111}In-DOTA-J415 elutes at 28 min after injection, and two main metabolites elute at 43 and 57 min after injection, respectively.

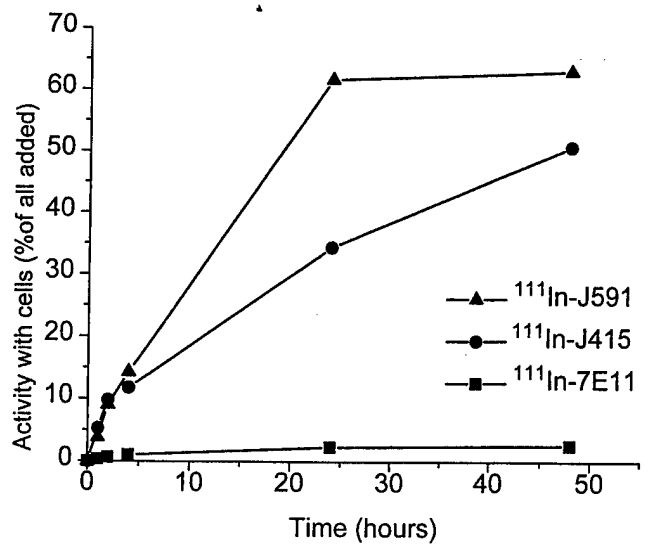

Fig. 9. Incorporation of ^{111}In-labeled cells by LNCaP cells. Petri dishes (8 cm^2) with confluent LNCaP cells were incubated with 37 KBq of either the ^{111}In-DOTA-J415 (●), ^{111}In-DOTA-J591 (▲), or ^{111}In-DTPA-7E11 (■). The samples were incubated at 37°C, and at various time points the location and the amount of cell-associated radioactivity were determined.

Table 1 *Inhibition constants for unlabeled J415, J533, J591, and 7E11 for the binding of ^{131}I-labeled J415, ^{131}I-labeled J533, and ^{131}I-labeled J591 binding to PMSA expressed by LNCaP cell membranes*

	IC_{50}s for displacing mAb (nM)			
Iodinated mAb	J415	J533	J591	7E11
^{131}I-labeled J415	1.5 ± 0.9	ND[a]	6.6 ± 4.5	ND
^{131}I-labeled J533	ND	2.3 ± 1.5	1.7 ± 1.3	ND
^{131}I-labeled J591	1.3 ± 0.9	7.7 ± 5.5	3.1 ± 1.5	ND

[a] ND, not displaced.

DISCUSSION

To understand the characteristics of and to select the best imaging/therapeutic agent, we studied binding characteristics and retention rates of the variously labeled mAbs using the LNCaP cell line, which expresses PMSA (Table 1).

The initial labeling of the three mAbs with ^{131}I, up to a specific activity of 350 MBq/mg, resulted in little or no apparent loss of immunoreactivity. Similarly, the conjugation of up to an average of five DOTA chelates per mAb enabled specific activities of up to 280 MBq ^{111}In/mg DOTA-J591 with no apparent loss of immunoreactivity. Site-specific modification of the antibody is sometimes required when this type of random DOTA coupling results in loss of immunoreactivity attributable to the presence of a lysine residue in the antigen binding domain. High specific activities are often required for accurate mAb characterization and particularly when large amounts of the radiotherapeutic agent are administered to a patient. J451 and J591 could be modified with sufficient DOTA to produce high specific activity ^{111}In- and ^{90}Y-labeled mAbs for both *in vitro* binding studies and eventual *in vivo* studies.

Early approaches to labeling mAbs with radiometals used DTPA, which in its dicyclic anhydride form could be conveniently coupled to mAbs (22). Unfortunately, this simple coupling chemistry produced a more labile chelate than bifunctional forms of the same unconjugated DTPA chelator (23). Macrocylic chelators have shown even higher kinetic stability (24), but they are even more time consuming to chemically synthesize (25). DOTA can be coupled directly to mAbs using simple chemistry and commercially available materials (20).

The reaction kinetics for ^{111}In and DOTA are longer than for DTPA, but an incubation period of 15 min can give high labeling yields. The DOTA chelator was immensely superior to DTPA in its ability to tightly chelate ^{111}In in the presence of an excess of competing ligand. This is in agreement with other studies (20, 26) and underlies the importance of using stable chelates with mAbs that can stay in circulation for prolonged periods of time in the presence of competing ligands (*e.g.*, transferrin). The higher stability of the ^{111}In-labeled DOTA complex relative to the ^{111}In-labeled DTPA complex also applies for the ^{90}Y complex (20, 26) and is an important prerequisite for radiolabeled mAbs used for either diagnosis or therapy because optimal tumor:nontumor ratios are often achieved after 2–4 days. Because ^{111}In-DOTA-J591 is stable to DTPA competition, it enables nonspecifically bound ^{111}In to be removed by challenging with DTPA and a simple column separation to yield a highly pure radiopharmaceutical.

High binding affinity between the mAb and the target antigen is another prerequisite to *in vivo* targeting of tumor antigens. The binding studies with the iodinated mAbs showed that two of three of these mAbs against $PSMA_{ext}$ (*i.e.*, J415 and J591) and 7E11 have similar nanomolar binding affinities. The use of intact and ruptured cells showed clearly that ^{131}I-labeled 7E11 binds to the intracellular domain of PMSA, consistent with other reports (13, 17). There was some binding of 7E11 to "intact" LNCaP cells, but that could be explained by the presence of a small population of cells ruptured during the trypsinization of the cells from the cell culture flasks and subsequent handling during resuspension. Because J591 recognized and specifically bound to twice the number of PSMA sites in permeabilized cells as opposed to intact cells, this suggests that only 50% of all cellular PSMA is exposed extracellularly. Also, 10–15% binding of 7E11 could be explained by the presence of a population of 5–7% of permeabilized cell in the "intact" cell preparation. This was confirmed in other studies that examined the binding and cellular uptake of the mAbs with plated LNCaP cells and showed a 7E11 uptake of 3–4% that of J415 and J591. This quantitative difference seen might explain why one group claims that the 7E11 binds to apparently intact LNCaP cells (27), whereas other groups report no such binding (13, 17, 18). Additionally, the Barren study (27) used cells that were scrapped from the monolayer, a procedure known to create significant cell rupture.

Effective systemic targeting of tumors has been achieved with both iodinated and metallochelated antibodies. A significant factor in selecting between the two approaches is in whether the antibody is internalized. In the case of an internalizing antibody, directly iodinated antibodies are metabolized within the cell, and the main metabolites of iodide and iodotyrosine are then freely released from the cell. Conversely, the metal chelate-labeled antibody is metabolized to leave a chelate-amino acid fragment that is typically not released from the cell and is trapped for further degradation. This effect can produce vastly different residence times for two differently labeled forms of the same antibody (28). In the LNCaP cell model, PSMA is known to be an internalizing surface bound glycoprotein (18). These studies clearly support the notion that metallolabeled mAbs are superior for cells expressing internalizable PSMA and that metabolites from the DOTA-mAb conjugate are not appreciably released from LNCaP cells.

In conclusion, both J415 and J591 have similar nanomolar affinities to PSMA as 7E11. Similarly, these two mAbs are far more readily bound and were internalized by live LNCaP cells than 7E11. The ^{111}In-labeled DOTA conjugates are able to associate more radioactivity with LNCaP cells than the comparable iodinated forms. The ^{111}In-labeled DOTA conjugates are also more stable to loss of ^{111}In than DTPA-7E11. These findings make DOTA-J415 and DOTA-J591 attractive candidates for further evaluation as either diagnostic or radiotherapeutic agents in patients with various cancers that express PMSA.

REFERENCES

1. Wingo, P. A., Ries, L. A., Rosenberg, H. M., Miller, D. S., and Edwards, B. K. Cancer incidence and mortality, 1973–1995: a report card for the U. S. Cancer (Phila.), *82:* 1197–1207, 1998.
2. Sanford, E., Grzonka, R., Heal, A., Helal, M., Persky, L., and Tyson, I. Prostate cancer imaging with a new monoclonal antibody: a preliminary report. Ann. Surg. Oncol., *1:* 400–404, 1994.
3. Meredith, R. F., Bueschen, A. J., Khazaeli, M. B., Plott, W. E., Grizzle, W. E., Wheeler, R. H., Schlom, J., Russell, C. D., Liu, T., and LoBuglio, A. F. Treatment of metastatic prostate carcinoma with radiolabeled antibody CC49. J. Nucl. Med., *35:* 1017–1022, 1994.
4. Slovin, S. F., Scher, H. I., Divgi, C. R., Reuter, V., Sgouros, G., Moore, M., Weingard, K., Pettengall, R., Imbriaco, M., El-Shirbiny, A., Finn, R., Bronstein, J., Brett, C., Milenic, D., Dnistrian, A., Shapiro, L., Schlom, J., and Larson, S. M. Interferon-γ and monoclonal antibody ^{131}I-labeled CC49: outcomes in patients with androgen-independent prostate cancer. Clin. Cancer Res., *4:* 643–651, 1998.
5. O'Donnell, R. T., De Nardo, S. J., Shi, X. B., Mirick, G. R., De Nardo, G. L., Kroger, L. A., and Meyers, F. J. L6 monoclonal antibody binds prostate cancer. Prostate, *37:* 91–97, 1998.
6. Kairemo, K. J., Rannikko, S., Nordling, S., Savalainen, S., Ahonen, A., Taavitsainen, M. J., and Alfthan, O. S. *In vivo* behavior of ^{111}In-labeled monoclonal anti-prostatic acid phosphatase antibody after intraprostatic and intravenous injections. J. Nucl. Biol. Med., *38* (Suppl. 1)*:* 151–155, 1994.
7. Deb, N., Goris, M., Trisler, K., Fowler, S., Saal, J., Ning, S., Becker, M., Marquez, C., and Knox, S. Treatment of hormone-refractory prostate cancer with ^{90}Y-CYT-356 monoclonal antibody. Clin. Cancer Res., *2:* 1289–1297, 1996.
8. Rydh, A., Ahlstrom, K. R., Widmark, A., Kahansson, L., Nilsson, S., Bergh, A., Damber, J. E., Stigbrand, T., and Hietala, S. Radioimmunoscintigraphy with a novel

monoclonal antiprostate antibody (E4). Cancer (Phila.), *80* (Suppl.): 2398–2403, 1997.

9. Murphy, G. P., Elgamal, A. A., Su, S. L., Bostwick, D. G., and Holmes, E. H. Current evaluation of the tissue localization and diagnostic utility of prostate specific membrane antigen. Cancer (Phila.), *83:* 2259–2269, 1998.
10. Sweat, S. D., Pacelli, A., Murphy, G. P., and Bostwick, D. G. Prostate-specific membrane antigen expression is greatest in prostate adenocarcinoma and lymph node metastases. Urology, *52:* 637–640, 1998.
11. Troyer, J. K., Beckett, M. L., and Wright, G. L., Jr. Detection and characterization of the prostate-specific membrane antigen (PSMA) in tissue extracts and body fluids. Int. J. Cancer, *62:* 552–558, 1995.
12. Wright, G. L., Grob, B. M., Haley, C., Grossman, K., Newhall, K., Petrylak, D., Troyer, J., Konchuba, A., Schellhammer, P. F., and Moriarty, R. Upregulation of prostate specific membrane antigen after androgen-depravation therapy. Urology, *48:* 326–334, 1996.
13. Lui, H., Moy, P., Kim, S., Xia, Y., Rajasekaran, A., Navarro, V., Knudsen, B., and Bander, N. H. Monoclonal antibodies to the extracellular domain of prostate-specific membrane antigen also react with tumor vascular endothelium. Cancer Res., *57:* 3629–3634, 1997.
14. Chang, S. S., Reuter, V. E., Heston, W. D. W., Bander, N. H., Grauer, L. S., and Gaudin, P. B. Five different anti-prostate-specific membrane antigen (PSMA) antibodies confirm PSMA expression in tumor-associated neovasculature. Cancer Res., *59:* 3192–3198, 1999.
15. Petronis, J. D., Regan, F., and Lin, K. Indium-111 capromab pendetide (ProstaScint) imaging to detect recurrent and metastatic prostate cancer. Clin. Nucl. Med., *23:* 672–677, 1998.
16. Troyer, J. K., Beckett, M. L., and Wright, G. L., Jr. Location of prostate-specific membrane antigen in the LNCaP prostate carcinoma cell line. Prostate, *30:* 232–242, 1997.
17. Troyer, J. K., Feng, Q., Beckett, M. L., and Wright, G. L. Biochemical characterization and mapping of the 7E11–C5.3 epitope of the prostate specific membrane antigen. Urol. Oncol., *1:* 29–37, 1995.
18. Lui, H., Rajasekaran, A. K., Moy, P., Xia, Y., Kim, S., Navarro, V., Rahmati, R., and Bander, N. H. Constitutive and antibody-induced internalization of prostate-specific membrane antigen. Cancer Res., *58:* 4055–4060, 1998.
19. Fraker, P. J., and Speck, J. C. Protein and cell membrane iodinations with a sparingly soluble chloramide, 1,3,4,6-tetrachloro-3a,6a-diphenylglycoluril. Biochem. Biophys. Res. Commun., *80:* 849–857, 1978.
20. Lewis, M. R., Raubitschek, A., and Shively, J. E. A facile, water-soluble method for modification of proteins with DOTA. Use of elevated temperature and optimized pH to achieve high specific activity and high chelate stability in radiolabeled immunoconjugates. Bioconjug. Chem., *5:* 565–576, 1994.
21. Lindmo, T., Boven, E., Cuttitta, F., Fedorko, J., and Bunn, P. A. Determination of the immunoreactive fraction of radiolabeled monoclonal antibodies by linear extrapolation to binding at infinite antigen excess. J. Immunol. Methods, *72:* 77–89, 1994.
22. Hnatowich, D. J., Layne, W. W., and Childs, R. L. The preparation and labeling of DTPA coupled albumin. J. Appl. Radiat. Isot., *33:* 327–332, 1982.
23. Roselli, M., Schlom, J., Gansow, O. A., Raubitschek, A., Mirzadeh, S., Brechbiel, M. W., and Colcher, D. Comparative biodistributions of yttrium- and indium-labeled monoclonal antibody B72.3 in athymic mice bearing human colon carcinoma xenografts. J. Nucl. Med., *30:* 672–682, 1989.
24. Meares, C. F., Moi, M. K., Diril, H., Kukis, D. L., McCall, M. J., Deshapnde, S. V., De Nardo, S. J., Snook, D., and Epenetos, A. A. Macrocyclic chelates of radiometals for diagnosis and therapy. Br. J. Cancer, *10* (Suppl.): 21–26, 1990.
25. Moi, M. K., Meares, C. F., and De Nardo, S. J. The peptide way to macrocyclic bifunctional chelating agents: synthesis of 2-*p*-nitrobenzyl-1,4,7,10-tetraazacyclododecane-*N,N',N'',N'''*-tetraacetic acid, and the study of its yttrium complex. J. Am. Chem. Soc., *110:* 6266–6267, 1998.
26. Camera, L., Kinuya, S., Garmestani, K., Wu, C., Brechbiel, M. W., Pai, L. H., McMurry, T. J., Gansow, O. A., Pastan, I., Paik, C. H., and Carrasquillo, J. A. Evaluation of the serum stability and *in vivo* biodistribution of CHX-DTPA and other ligands for yttrium labeling of monoclonal antibodies. J. Nucl. Med., *35:* 882–889, 1994.
27. Barren, R. J., Holmes, E. H., Boynton, A. L., Misrock, S. L., and Murphy, G. P. Monoclonal antibody 7E11.C5 staining of viable LNCaP cells. Prostate, *30:* 65–68, 1997.
28. Stein, R., Chen, S., Haim, S., and Goldenberg, D. M. Advantage of yttrium-90-labeled over iodine-131-labeled monoclonal antibodies in the treatment of a human lung carcinoma xenograft. Cancer (Phila.), *80* (Suppl. 12): 2636–2641, 1997.

APPENDIX- B

Figure 1: **Tumor/Blood and Tumor/Muscle Ratios of ^{131}I and ^{111}In-Labeled Mabs (J591, J415, 7E-11) in Nude Mice with LNCaP tumors**

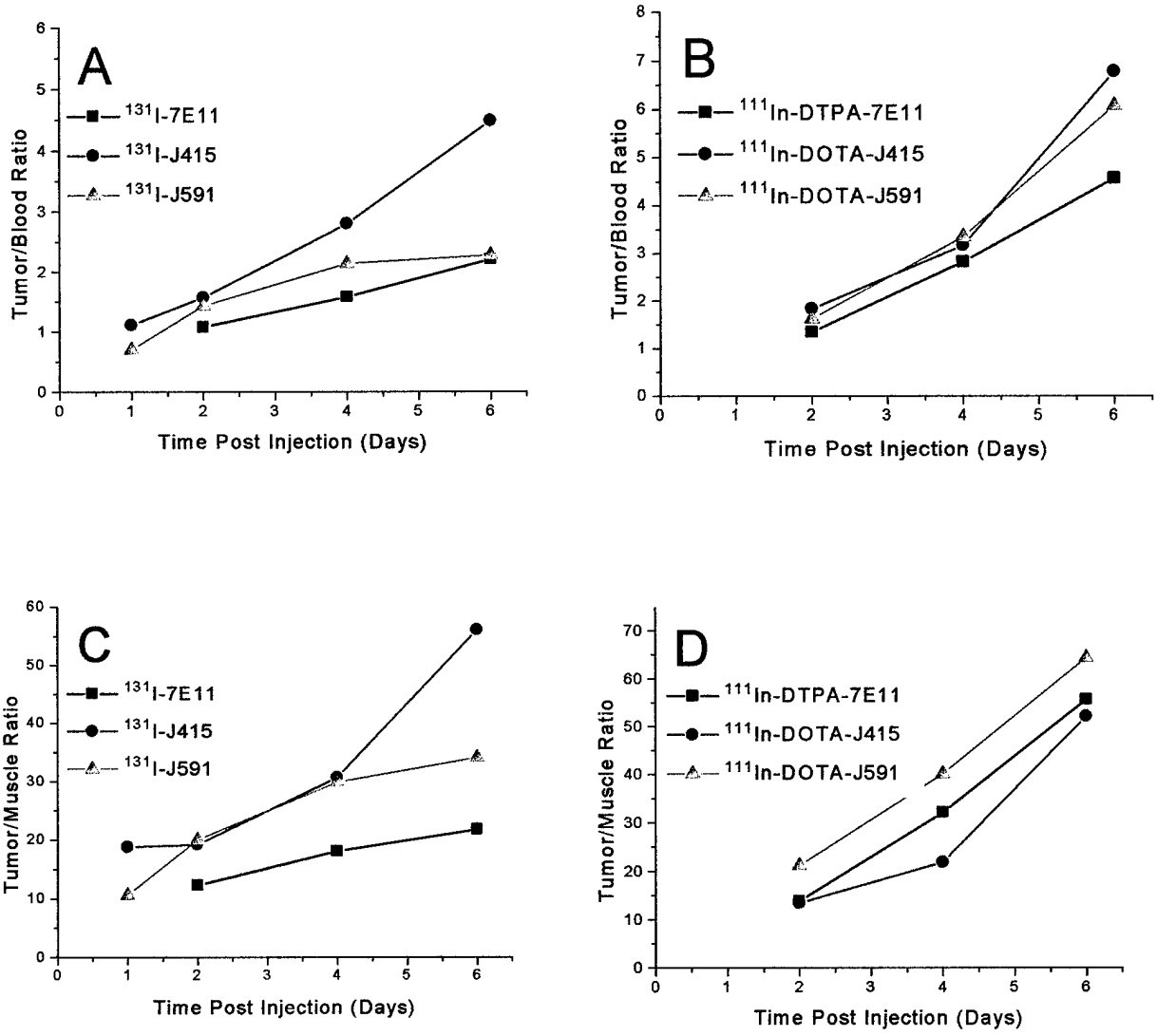

Figure 2: Gamma Camera Images of a Nude Mouse with LNCaP tumor. Images were obtained with a pin-hole collimator on days 1,2,3,4, and 6 post injection of ^{111}In-DOTA-J591.

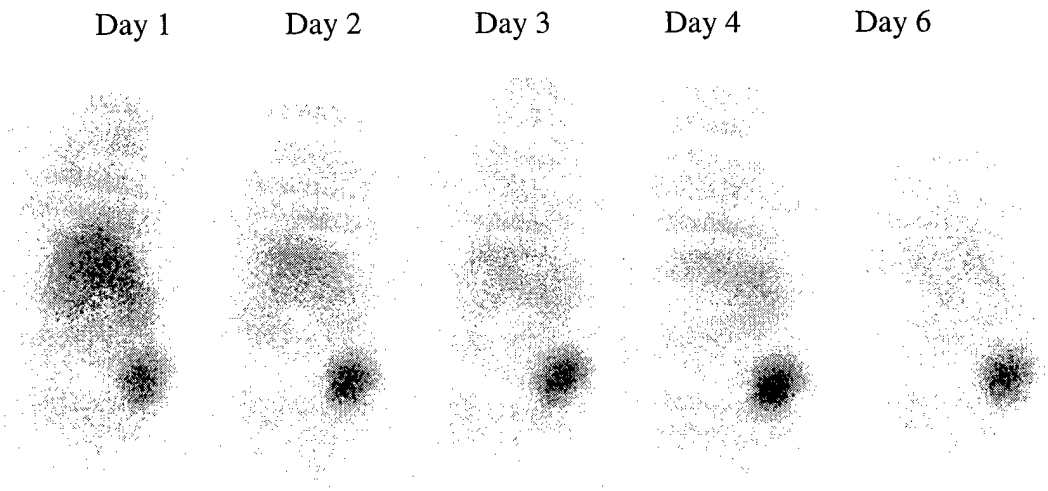

Figure 3A: Blood Clearance of Radiolabeled J591 MAb.

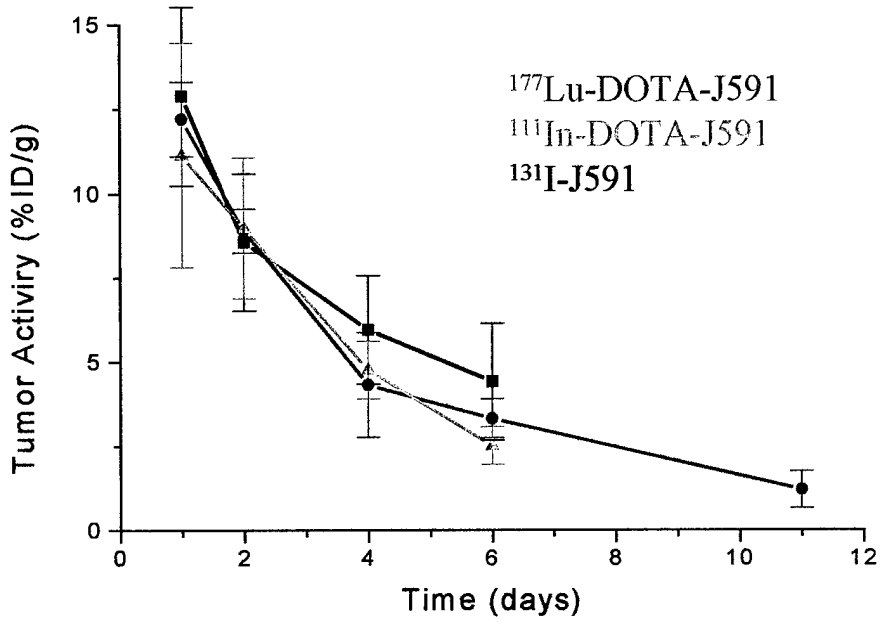

Figure 3B: Tumor Uptake of Radiolabeled J591 MAb.

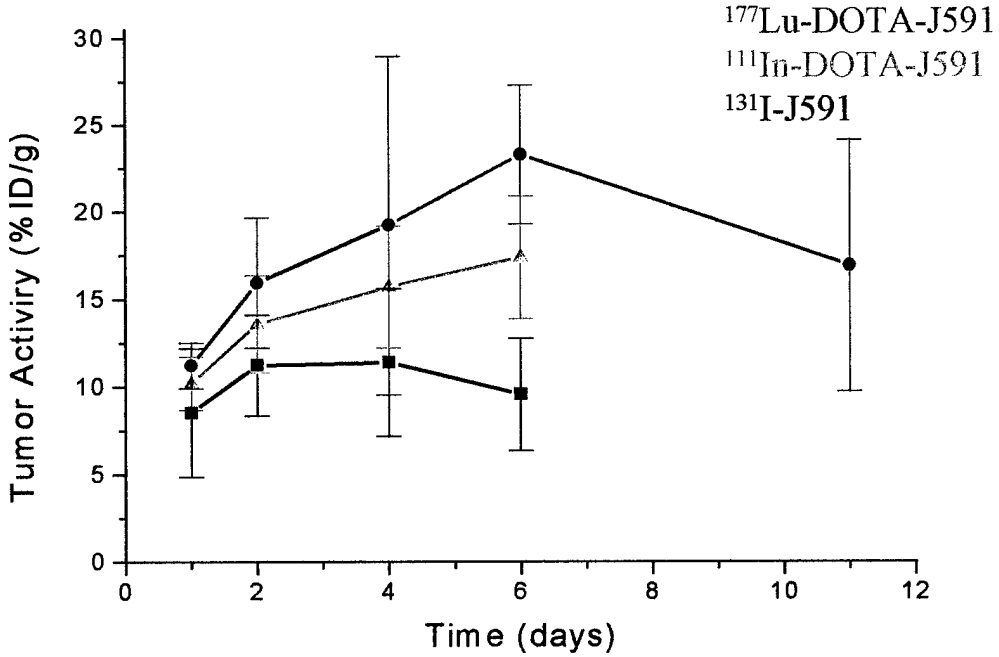

Figure 4: Radioimmunotherapy of nude mice bearing LNCaP tumors using ^{131}I-J591 MAb.

Compared to untreated controls, anti-tumor effect of ^{131}I-J591 was dependent on the dose. At 100μCi dose, there was some delay or reduction in tumor size. But at 300μCi dose, all the mice had a significant reduction in tumor size. 2/5 mice in cotrol group died in 4 weeks and the remaining 3 survived more than 6 weeks. With I-131, while there was reduction in tumor size, the % survival also decreased compared to controls. Interestingly, mice that received 100μCi intraperitoneally survived longer than 6 weeks.

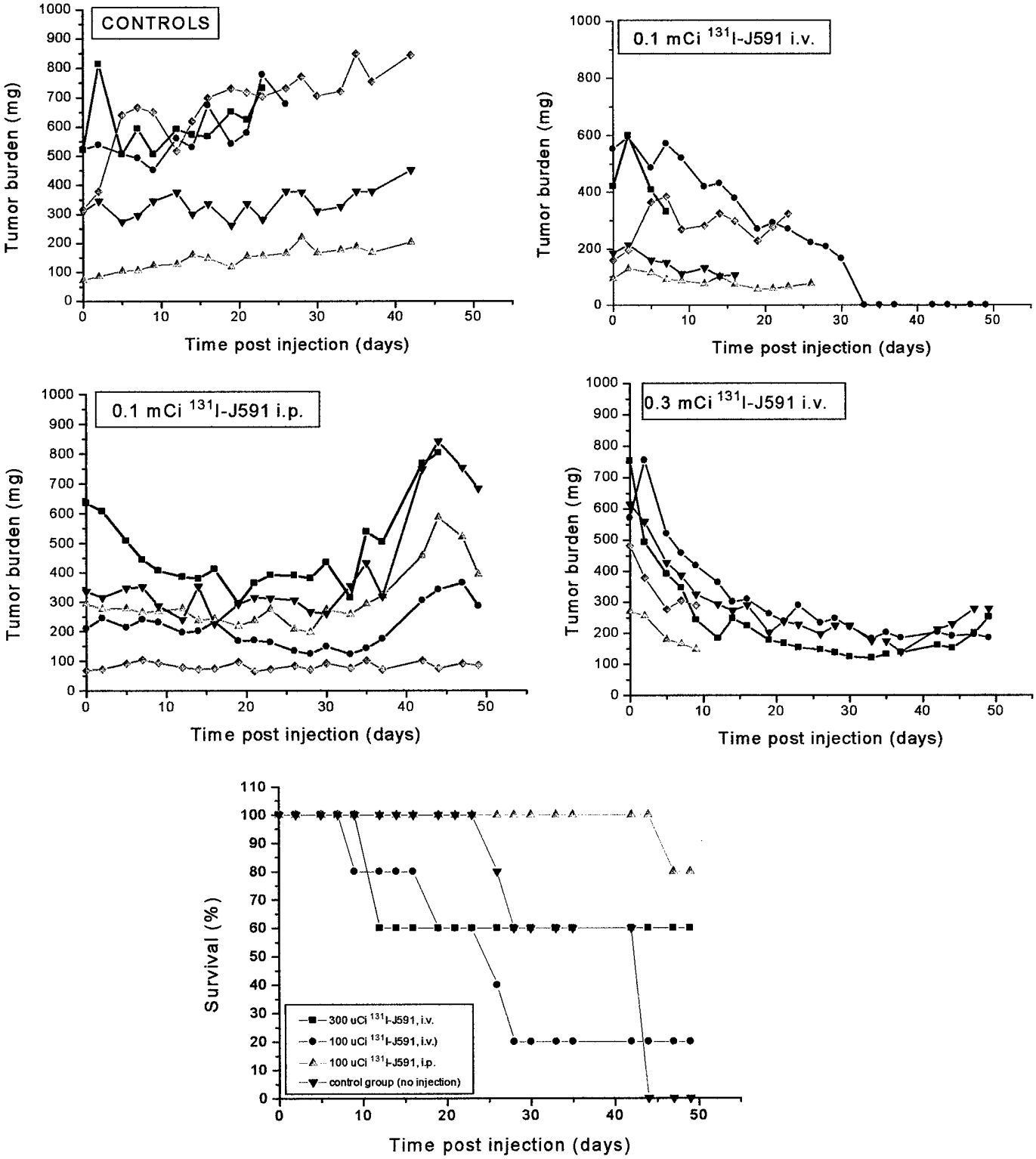

Figure 5A: Radioimmunotherapy of nude mice bearing LNCaP tumors: ^{131}I-J591 Vs. ^{90}Y-J591 MAb.

(5-7 mice/ group; 4 groups total)

Compared to untreated controls, the anti-tumor effect of ^{90}Y-J591 (35μCi) was similar to that of ^{131}I-J591 (300μCi). Mice that received a second injection of ^{90}Y-J591 (35μCi) showed further reduction in tumor size.

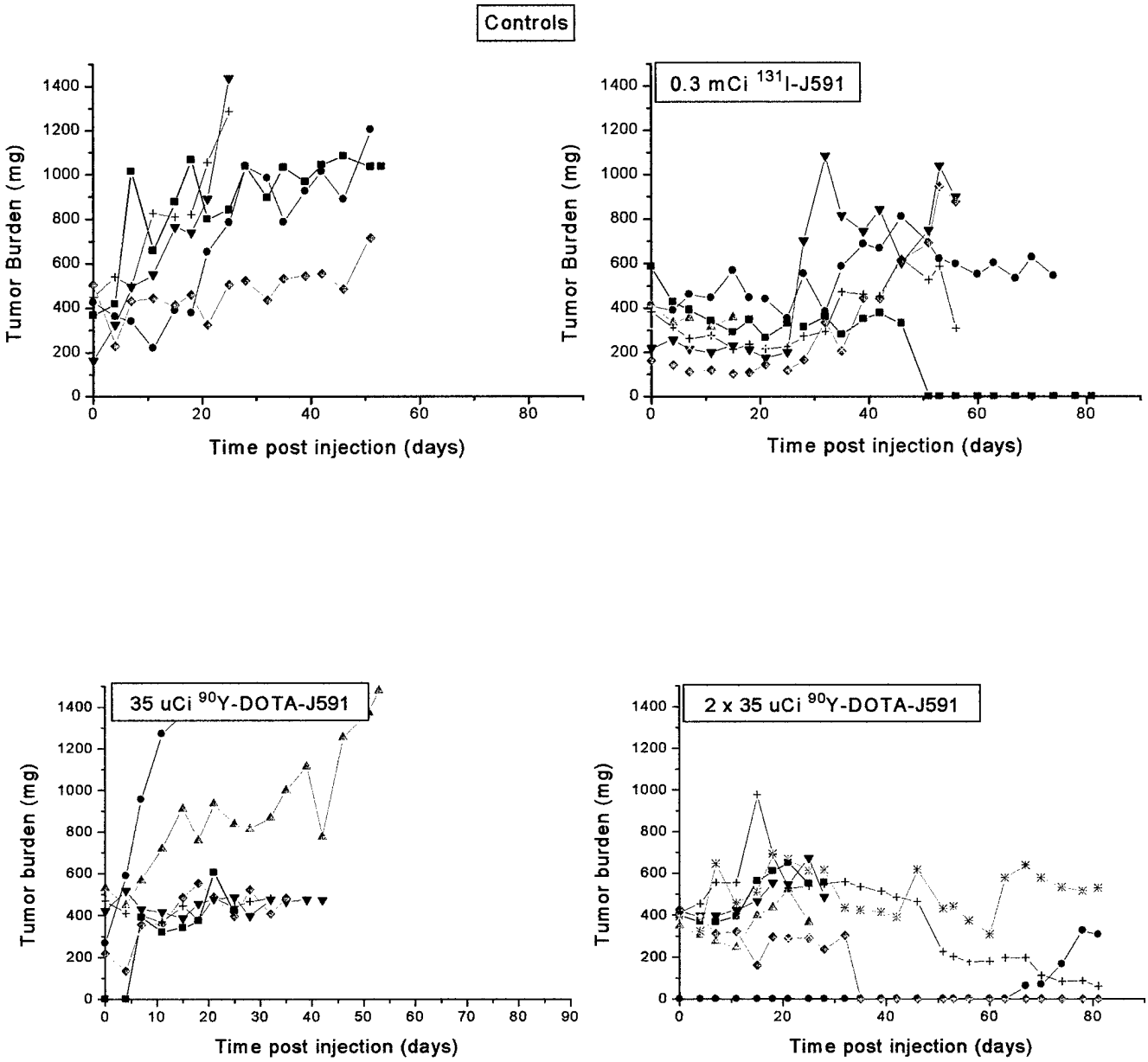

2 injections day 0 and day 21

Figure 5B: Treatment of nude mice with LNCaP tumors using ^{90}Y–DOTA-J591:

Effect on total body mass (weight of the animal)

There was a gradual reduction (20% within 6-8 weeks) in the total body mass of mice both in control group and mice that received only 30μCi of ^{90}Y-DOTA-J591. However, following second injection of the treatment (at the same dose level), there was a gradual recovery of total body mass. With ^{131}I-J591 (at 300μCi), there was some recovery of body mass, but most of the animals died within 8-10 weeks.

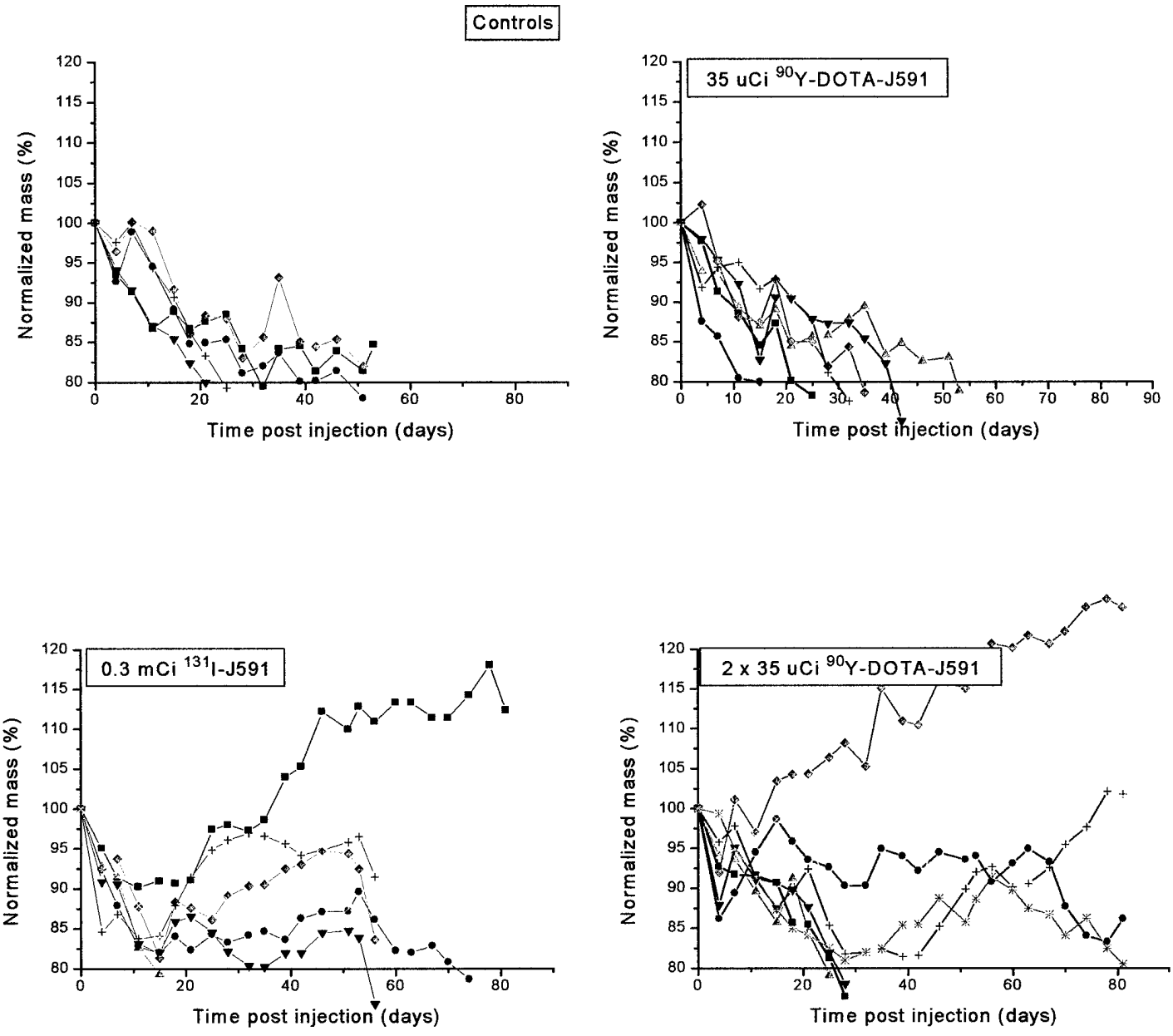

Figure 6 A: **Radioimmunotherapy of nude mice bearing LNCaP tumors using ^{90}Y-DOTA-J591 MAb.** (Comparison with **untreated controls** and mice treated with **non-specific antibody (F23))**

Mice were treated with 3 different doses (30, 60 and 90μCi) of ^{90}Y-DOTA-J591 MAb. The mice in each group received repeat injections at the same dose level 3 times (days 0, 28 and 56). Mice in control group also received non-specific antibody 3 times. Total 5 groups; 6-7 mice/group

The antitumor effect of ^{90}Y-DOTA-J591 MAb was dose dependent (greatest response at 90μCi (Figure 6B)) and very specific sice control mice (that received non-specific antibody) had an uncontrolled tumor growth.

Compared to control groups, mice that received 30 and 60μCi of ^{90}Y-DOTA-J591 MAb had a significantly longer survival rate (Figure 6B)

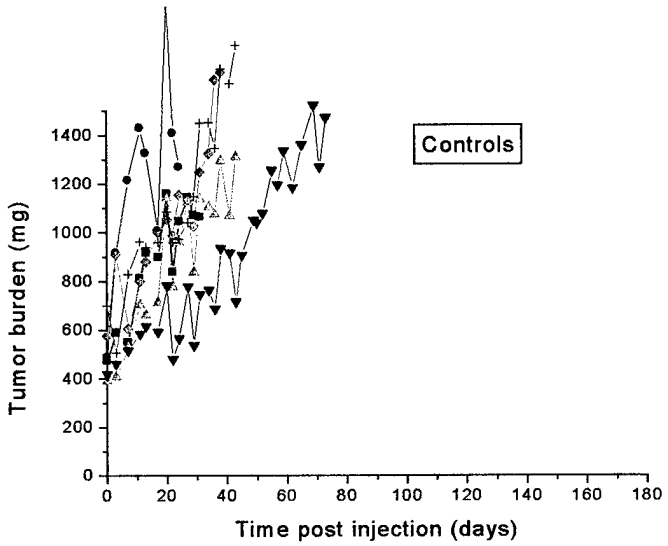

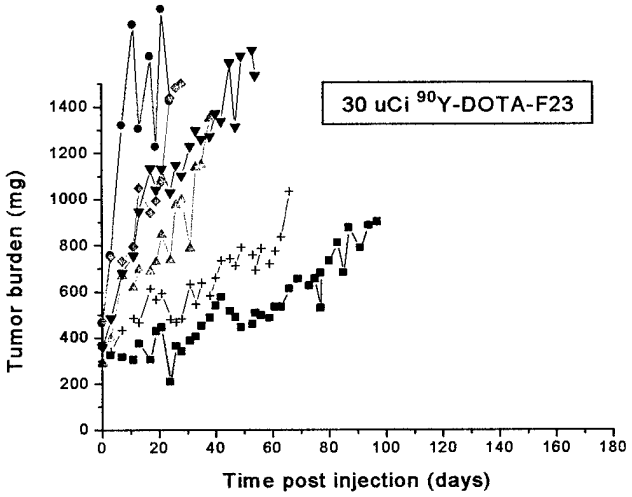

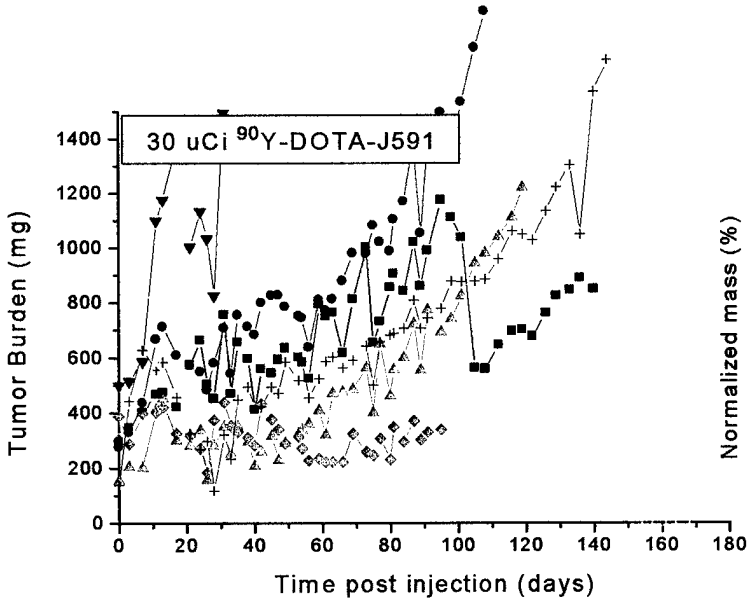

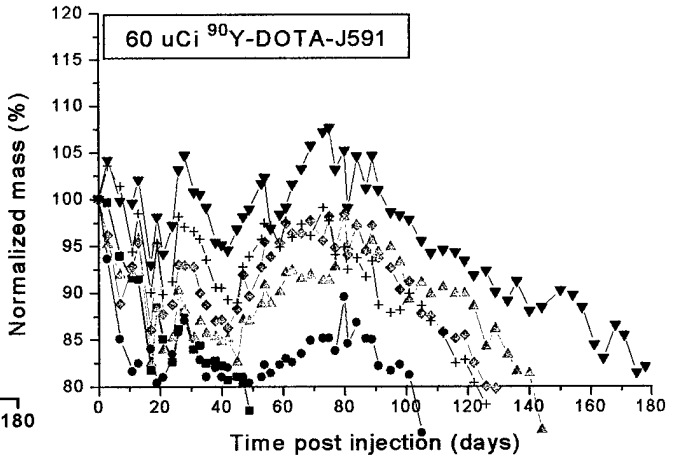

Figure 6 B: **Radioimmunotherapy of nude mice bearing LNCaP tumors using ^{90}Y-DOTA-J591 MAb.**

(Comparison with **untreated controls** and mice treated with **non-specific antibody (F23))**

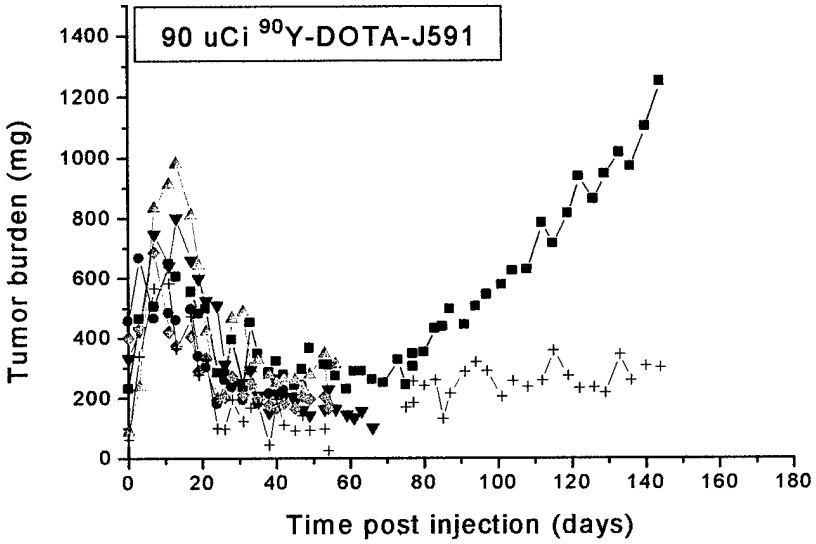

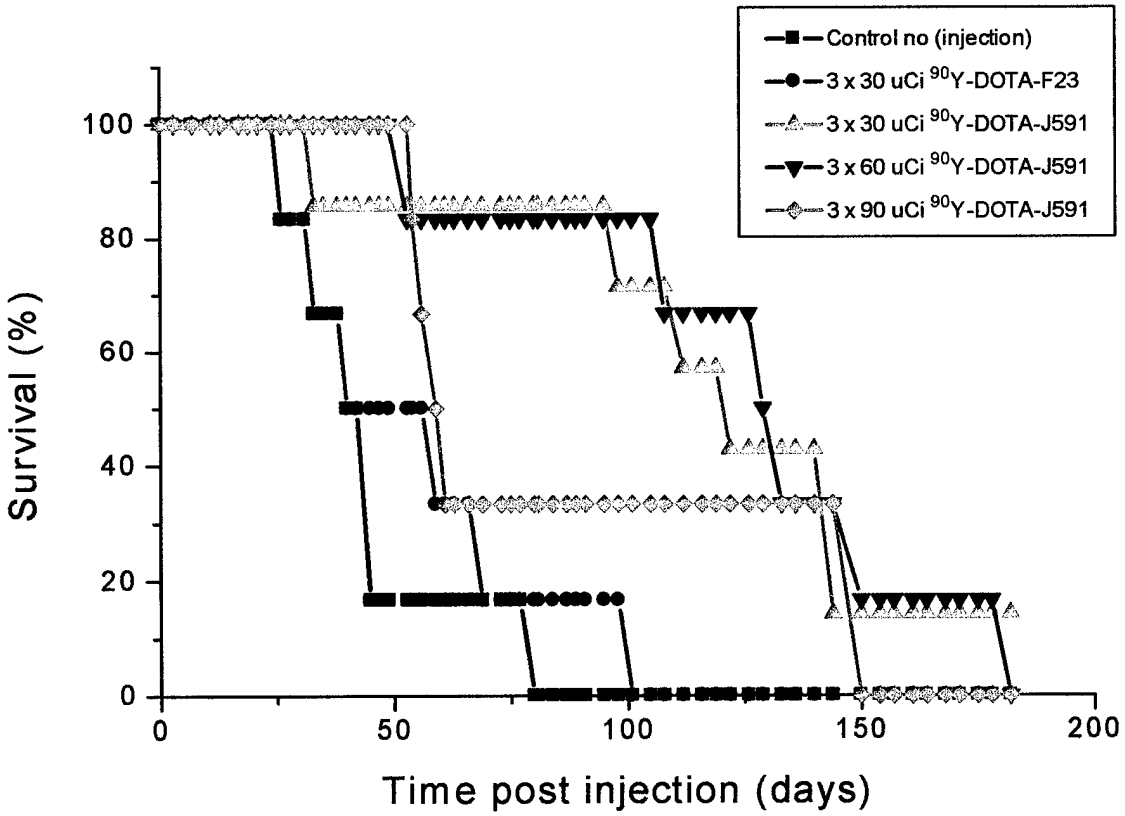

Figure 6C: Treatment of nude mice with LNCaP tumors using ^{90}Y–DOTA-J591:

Effect on total body mass (weight of the animal)

There was a gradual reduction (20% within 6-8 weeks) in the total body mass of mice both in control group. Mice that received repeated(days 0, 28, and 56) treatment doses of 30 and 60μCi of ^{90}Y-DOTA-J591 showed a gradual increase in total body mass compared to control mice.

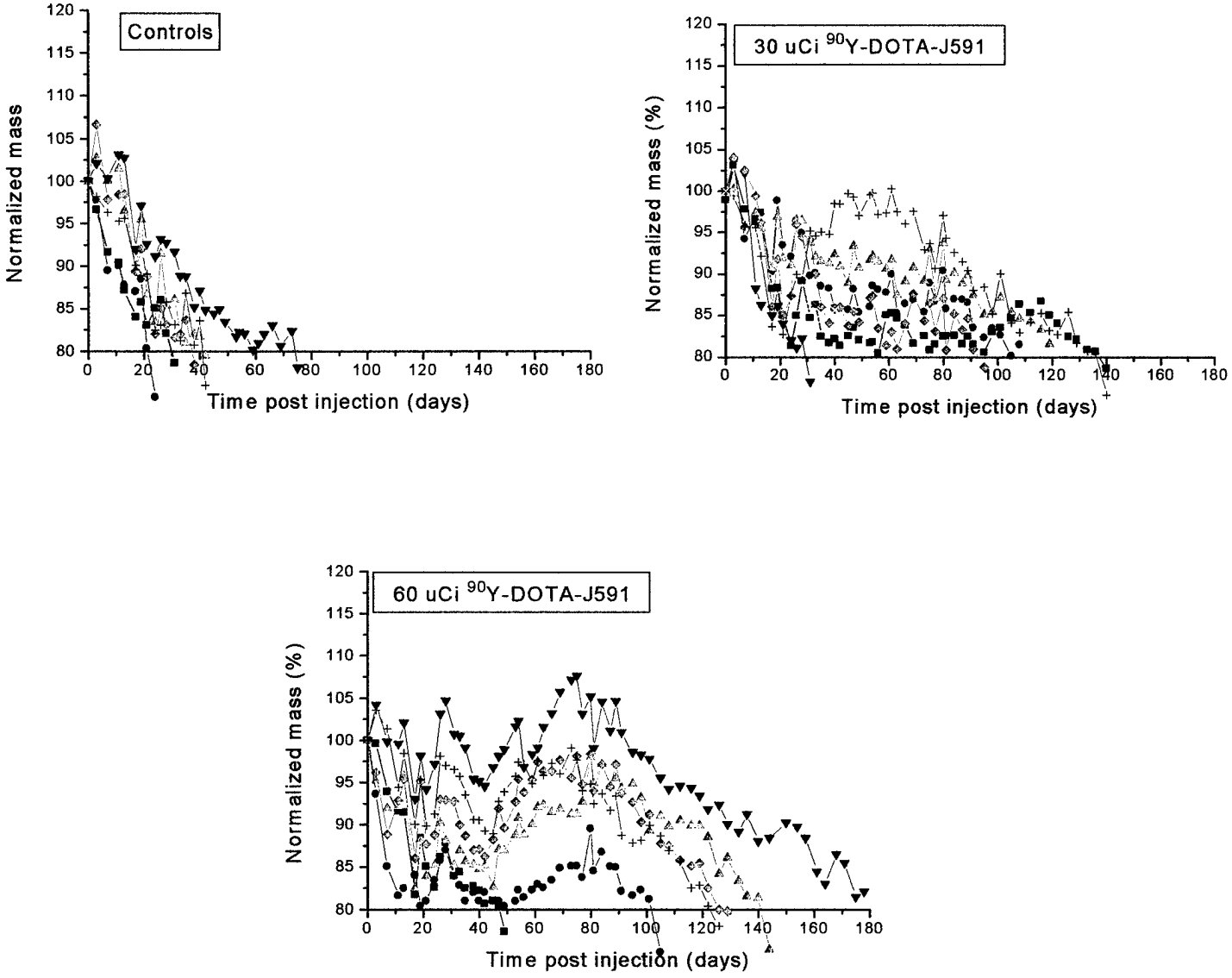

Figure 7: Radioimmunotherapy of nude mice bearing LNCaP tumors using ^{90}Y-DOTA-J591

Dose –response (anti-tumor effect) relationship and relative toxicity.

3 groups (n= 4-5) of mice were injected with different doses (150, 200, and 300μCi) of ^{90}Y-DOTA-J591. There was a significant reduction in tumor volume with all 3 dose levels. However, at 150 μCi dose level, 5 weeks after the treatment dose, tumors started to grow again (tumor vilume increased 2-times the baseline value. In contrast, most of the mice at 200-300 μCi dose level died within 3-4 weeks following the treatment dose suggesting that these dose levels are associated with increased toxicity.

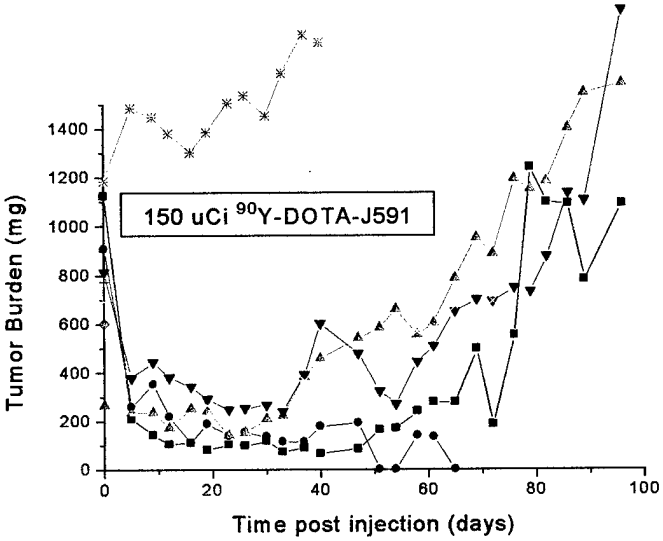

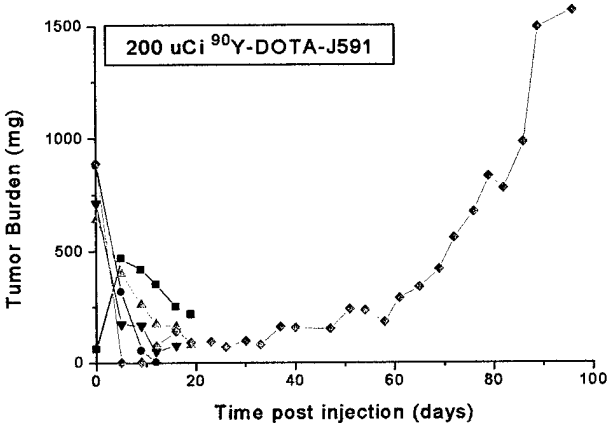

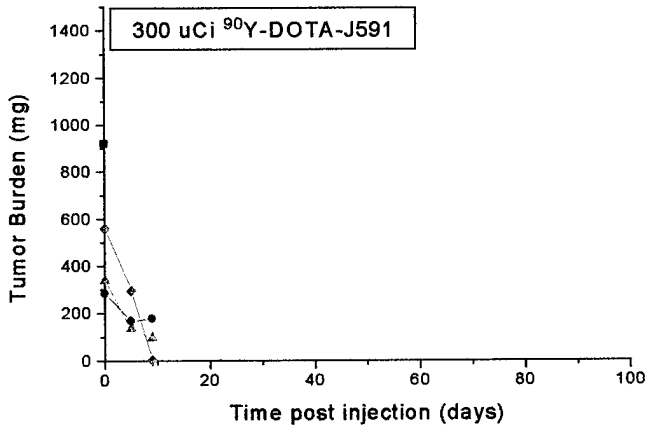

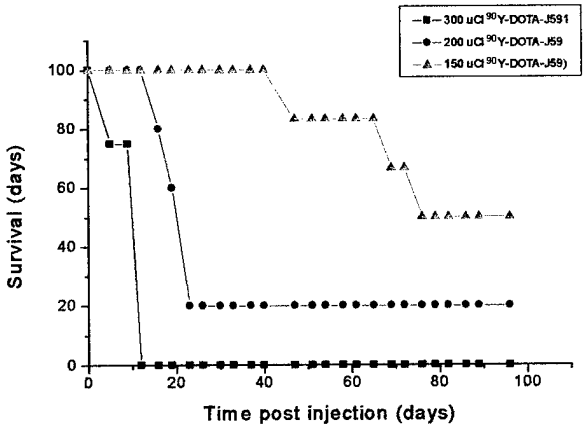

Figure 8: Radioimmunotherapy of nude mice bearing LNCaP tumors:

^{90}Y-DOTA-J591 Vs. ^{90}Y-DOTA-J415

The anti-tumor effect of ^{90}Y-DOTA-J591 was compared to that of ^{90}Y-DOTA-J415. Two groups (n=7/group) of mice received 60μCi of labeled MAb. Mice in each group received a total of 3 doses (at the same dose level) over a period of 2 months (Days 0, 35 and 63). For comparison, a control group received no treatment.

Compared to controls, both antibody (J591 and 415) preparations had a significant anti-tumor response. However, ^{90}Y-DOTA-J591 response appeared to be greater and more consistent. In addition, the % survival with Y-90 labeled J591 and J415 was significantly greater compared to that of controls.

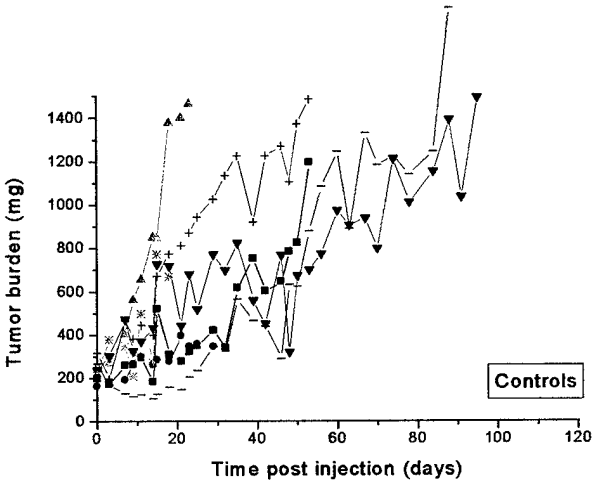

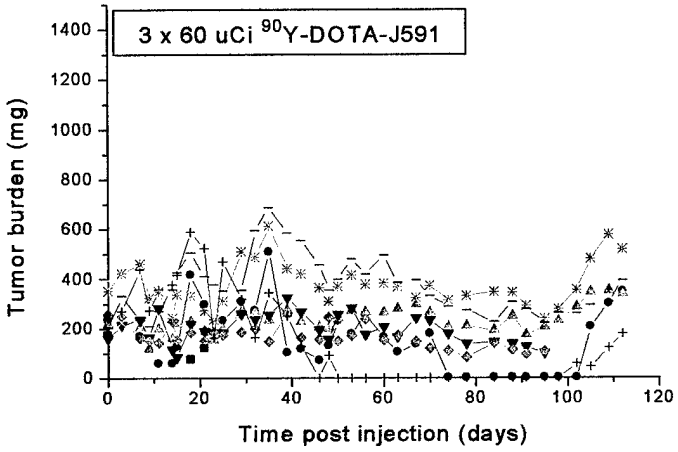

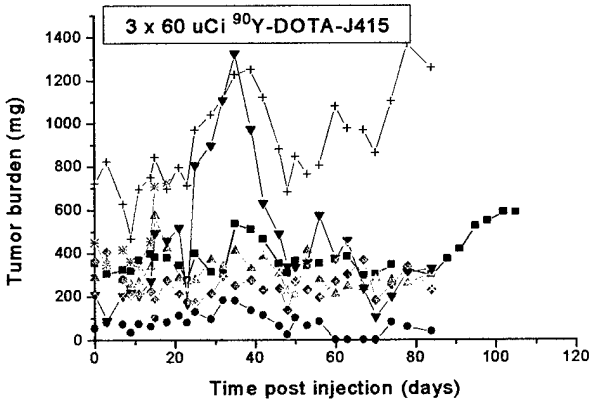

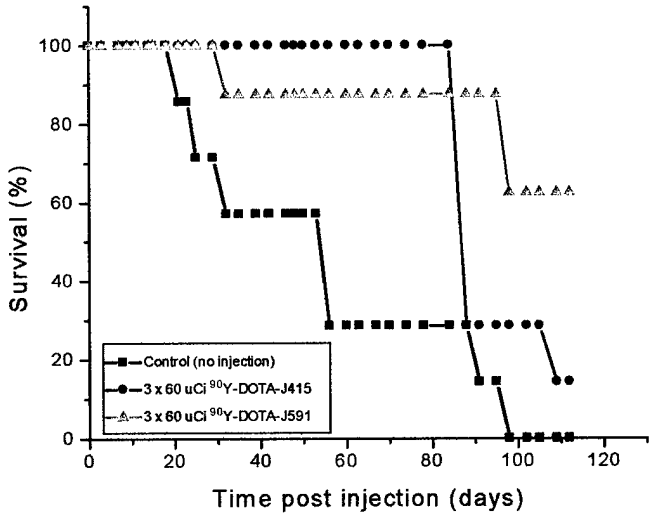

Figure 9A: Radioimmunotherapy of nude mice with LNCaP tumors using ^{177}Lu-DOTA-J591.

3 groups (n=6-7/group) of mice were injected with a single dose of 100, 200, and 400μCi of ^{177}Lu-DOTA-J591. A control group (n=7) received no treatment. With 100 μCi, there was a delay in tumor growth. But at 200-400 μCi dose levels, the anti-tumor effect was significant. 6-8 weeks following treatment, tumors started frowing slowly There was greater survival rate at 200μCi and is less toxic

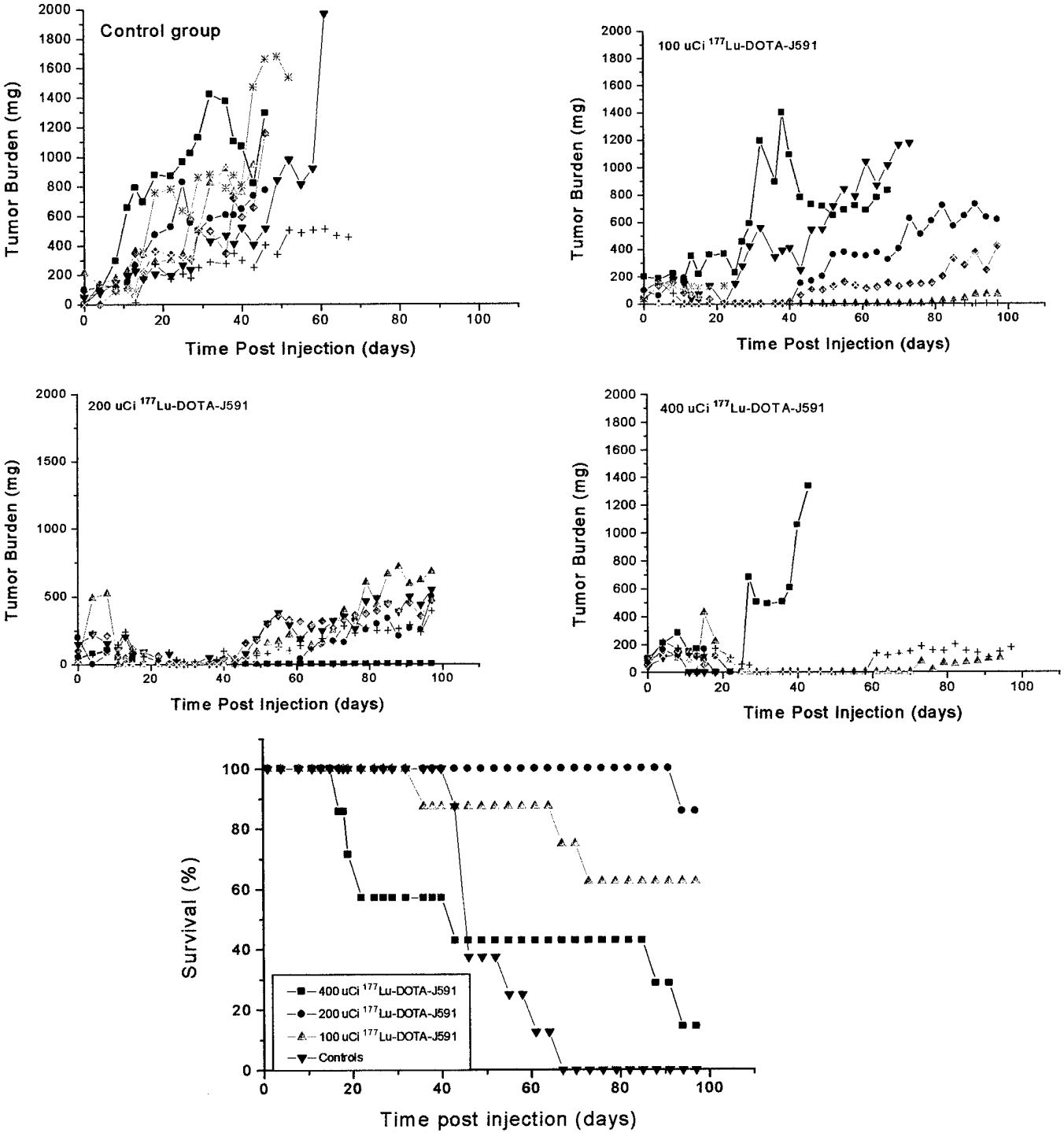

Figure 9B: Treatment of nude mice with LNCaP tumors using ^{177}Lu-DOTA-J591:

Effect on total body mass (weight of the animal)

There was a gradual reduction (20% within 6-8 weeks) in the total body mass of mice in the control group. In contrast, mice treated with 200μCi of 177Lu-DOTA-J591 there was no significant reduction in the body mass over a period of 8-10 weeks. However, at 400μCi dose level 50% of the mice had a gradual decline in the body mass and died within 3-6 weeks.

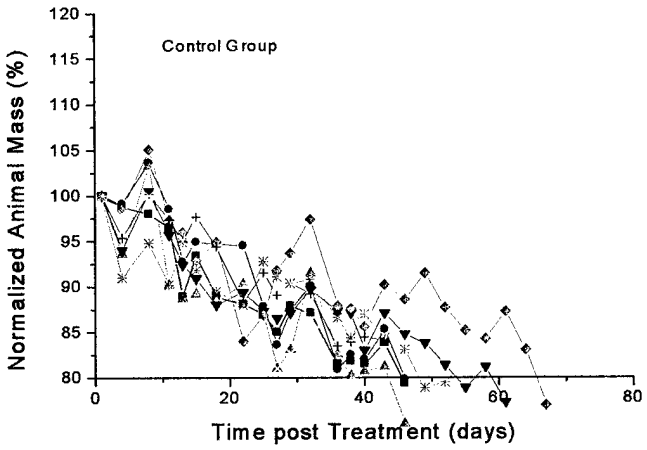

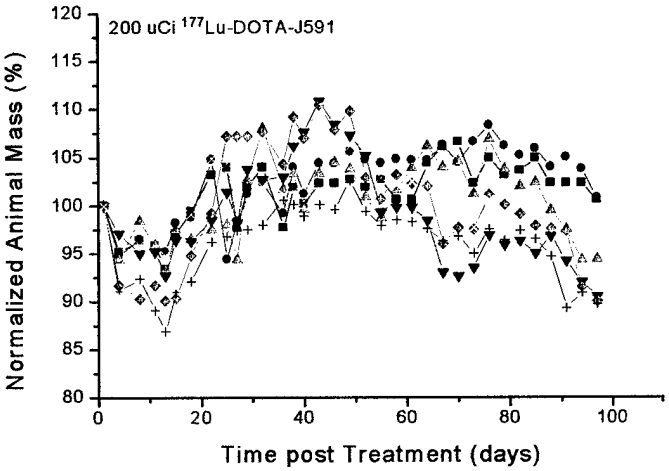

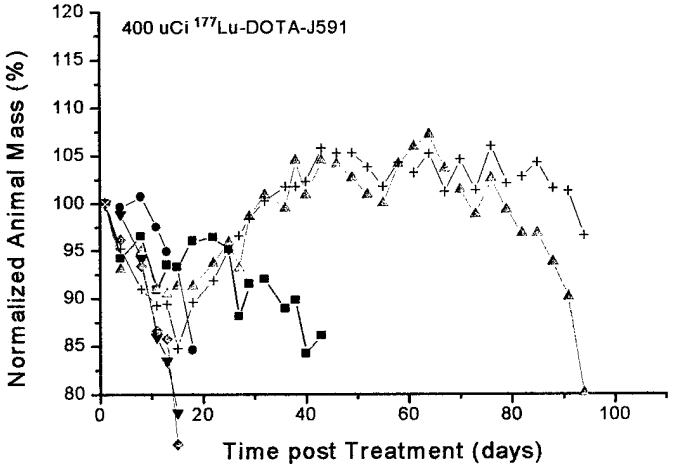

BIBLIOGRAPHY

1. Vallabhajosula S. Kostakoglu L. Goldsmith S.J. Bastidas D, Navarro V Gomez D. Bander NH. Monoclonal antibody J591 specific to the extracellular domain of PSMA: A new agent for radioimmunodiagnosis (RID) and radioimmunotherapy. J Nucl Med 1998;39(5 Suppl):77P-78P (Abstract).
2. Smith-Jones PM, Vallabhajosula S, Hunter CJ, et al. Monoclonal Antibodies (MAb) specific to extracellular Domain of PSMA: in vitro studies. J Nucl Med 1999; 40: (5suppl): 226p (abstract).
3. Smith-Jones PM, Vallabhajosula S, Bastidas D, et al. In vivo evaluation of I-131 labeled MAbs specific for extracellular Domain of PSMA. J Nucl Med 1999; 40: (5suppl): 225p (abstract).
4. Vallabhajosula S, Smith-Jones PM, Bastidas D, et al. Preclinical studies of radiolabeled J591 MAb specific for extracellular domain of PSMA: Comparison with ProstaScint. Eur J Nucl Med 1999; 26(9):1212 (Abstract).
5. Smith-Jones PM, Vallabhajosula S, Bastidas D, et al. Preclinical studies with ^{131}I and ^{111}In labeled MAbs, specific for the intracellular or extracellular domains of PSMA. J Label Comp Radiopharma 1999; 42:suppl 1,s701-703 (Abstract).
6. Smith-Jones PM, Navarro V, Bander N, Goldsmith SJ, Vallabhajosula S. Uptake and Metabolism of ^{111}In and ^{131}I labeled Anti-PSMA Monoclonal Antibodies by Prostate Carcinoma cells. J. Nucl Med 2000;41:(5 suppl):142p (Abstract).
7. Smith-Jones PM, Vallabhajosula S, Navarro V, Goldsmith SJ, Bander NH. ^{90}Y-huj591 MAb specific to PSMA: Radioimmunotherapy (RIT) studies in nude mice with prostate cancer LNCaP tumor. Eur J Nucl Med 2000; 27(8):951 (Abstract).
8. Smith-Jones PM, Vallabhajosula S, Goldsmith SJ, Navarro V, Hunter CJ, Bastidas D, Bander NH. In vitro Characterization of Radiolabeled Monoclonal Antibodies Specific for the Extracellular Domain of Prostate-specific Membrane Antigen. Cancer Res 2000; 60:5237-5243.

Personnel Who Received Salary:

Shankar Vallabhajosula, Ph.D.

David Gomez, Ph.D.

Diego Bastidas, B.S.

Vincent Navarro, B.S.

St. Omer, B.S.